LA-UR-84-512

CONF-8402516--1

Los Alamos National Laboratory is operated by the University of California for the United States Department of Energy under contract W-7405-ENG-36

TITLE: MICROTHEORY OF COLLISIONLESS SHOCK CURRENT LAYERS

LA-UR--84-512

DE84 007500

AUTHOR(S): D. WINSKE

SUBMITTED TO:

PROCEEDINGS OF THE CHAPMAN CONFERENCE ON COLLISIONLESS SHOCK WAVES IN THE HELIOSPHERE, NAPA VALLEY, CA, FEBR. 20-24, 1984

DISCLAIMER

Los Alamos Los Alamos National Laboratory
Los Alamos, New Mexico 87545

FORM NO 836 R4
ST NO 2629 5/81

MICROTHEORY OF COLLISIONLESS SHOCK CURRENT LAYERS

D. Winske
Los Alamos National Laboratory, Los Alamos, NM 87545

Abstract

The present status of understanding of microscopic dissipation processes in the current layer of collisionless shocks is reviewed. The emphasis is on cross-field current-driven instabilities and their importance in quasiperpendicular shocks, although other processes which arise in quasiparallel shocks are also discussed. A general prescription is given for calculating turbulent heating and resistivity in shocks.

I. Introduction

In collisionless shocks the directed flow energy in the upstream region is converted to thermal energy in the downstream region over distances that are much shorter than the classical mean free path of the flowing particles. A good example of such shocks is the earth's bow shock, where the scale length of the transition region between the upstream and downstream states is less than several hundred kilometers, while the mean free path of the solar wind ions is on the order of 10^7 kilometers (e.g., see reviews by Greenstadt and Fredricks (1979) and Kennel (this meeting)). The bow shock transition is very distinct, and thus most easily seen, near the portion of the shock where the upstream magnetic field is nearly perpendicular to the shock normal ("perpendicular shock"). In contrast, near the portion of the shock where the shock normal and upstream magnetic field are nearly parallel ("parallel shock"), the transition is obscured by large magnetic field fluctuations which extend for thousands of kilometers upstream and downstream from the point where the plasma properties change abruptly. It has been recognized for many years that the "collisionless" process by which some of the flow energy is dissipated is due to the interaction of the solar wind particles with plasma waves generated as a result of microinstabilities which arise because of various sources of free energy in the system (e.g., relative drifts between the plasma components, non-Maxwellian velocity distributions, gradients in density, temperature, magnetic field, etc.). The study of dissipation processes in collisionless shocks then has been aimed at identifying the possible sources for instabilities, working out the properties of the unstable modes (both in their linear and nonlinear behavior) and then analyzing their effects on the plasma in terms of bulk heating and particle acceleration and on the current and field structure in terms of an "anomalous" resistivity.

A number of good reviews of dissipation processes in shocks already exist. The state of the art up to 1973 is best summarized in the article of Biskamp (1973), a very thorough review of all aspects of collisionless shocks. Instabilities related to the earth's bow shock have been considered by Greenstadt and Fredricks (1974). Galeev (1976) has reviewed the subject of heating in collisionless shocks, especially with regard to ion sound turbulence. Papadopoulos (1977) has discussed the instabilities which develop from a current along a magnetic field with applications to magnetospheric and ionospheric phenomena. Instabilities which develop from cross-field currents that occur in laboratory shocks have been considered by Davidson and Krall (1977).

Wu (1982) has emphasized the underlying physical processes for dissipation at both quasiparallel and quasiperpendicular shocks with a limited discussion of the instabilities themselves. Finally, Wu et al. (1984) have reexamined the instabilities relevant to quasiperpendicular shocks and updated much of the theory to apply to supercritical shocks where reflected ions become important. There are also good discussions in textbooks of instabilities (e.g., Krall and Trivelpiece, 1973; Hasegawa, 1975) and their effects on shocks, (e.g., Tidman and Krall, 1971).

The purpose of the present review is to update from Biskamp (1973) what is known about the various instabilities which are thought to be responsible for the dissipation in collisionless shocks. This will include the current status of the linear, nonlinear, and transport (e.g., heating) properties of the instabilities in general and with application to shocks in particular. This type of review is needed because much progress has been made in the last decade and many of the results are not found in space physics journals. A review of this kind is also appropriate because recent advances in the construction of large computers and formulation of numerical simulation methods (e.g., implicit codes) make a reinvestigation of some of the unanswered questions feasible today on a scale which would have been impossible ten years ago.

In this review we will restrict our attention primarily to current-driven instabilities in the transition layer. These have been the most widely studied and their importance for dissipation in quasiperpendicular shocks is well known. Our understanding of dissipation processes (as well as most other phenomena) at quasiparallel shocks is much more rudimentary and will be discussed only briefly here. (Also see reviews at this meeting by Greenstadt and Quest). Instabilities and associated particle behavior (e.g., acceleration) in the upstream region will be treated in other reviews (e.g., Thomsen, Klimas), as will manifestations of the instabilities (i.e., wave observations, heating as derived from particle distributions) (Gurnett, Robson).

The plan of this review is as follows. In Sec. II the basic concepts of the instability analysis are enumerated. The field and current structure of a quasiperpendicular shock is first described and the role of plasma instabilities is identified. The need for microturbulent dissipation is then illustrated through observations of plasma heating at shocks. How the effects of the instabilities enter in is recalled by means of the quasilinear equations for the macroscopic quantities. A basic prescription involving four steps is then laid out. The first step involves the identification of the various instabilities from their sources of free energy (which may vary across the shock layer) and their categorization into mode types (electromagnetic or electrostatic) and frequency ranges. Linear analysis is the next step; its essential features and ultimate goals are delineated. The third step is nonlinear analysis. Various approaches, including simulation methods, are outlined. In the final step the results of the previous steps are fed back into the quasilinear equations to give rates for plasma heating and expressions for the resistivity. While it sounds (and is) straightforward, very few calculations for actual shocks have been done in detail.

In Sec. III the different steps of this process are analyzed for various modes. First, the instabilities are identified and then subdivided into high frequency (electrostatic) modes and low frequency (electromagnetic) modes. The electrostatic modes include the much studied ion acoustic instability and the somewhat neglected electron cyclotron drift instability. The electromagnetic modes considered include the ion-ion instability, the modified two stream (also known as the kinetic cross-field streaming) instability, and the lower hybrid drift instability. For each instability we summarize the current state of linear and nonlinear theory, simulations, and transport properties, especially with regard to shock-like geometries. In addition, we briefly discuss other instabilities and dissipation processes which may contibute, but which have been studied much less thoroughly.

Finally, in Sec. IV we summarize the overall status of microtheory, where we stand today, how far we have advanced in the last ten years, and where we hope to be in the future. We also discuss the strengths and weaknesses of the present approaches and how they are being improved. Finally, we point out what is needed to increase our level of understanding of collisionless shocks in the next few years.

II. Basic Concepts

A. Notation and geometry

For convenience we first collect the definitions of the symbols used throughout the text. We let e_α=charge, m_α=mass, n_α=density, T_α=temperature, $v_\alpha=(2T_\alpha/m_\alpha)^{1/2}$=thermal speed, $\Omega_\alpha=|e_\alpha|B/m_\alpha c$=cyclotron frequency, $\beta_\alpha=8\pi n_\alpha T_\alpha/B^2$= ratio of plasma pressure to magnetic pressure, $v_{n\alpha}=\varepsilon_{n\alpha}v_\alpha^2/2\Omega_\alpha$=diamagnetic drift speed, $\rho_\alpha=v_\alpha/\Omega_\alpha$=gyroradius, and $\lambda_{D\alpha}=v_\alpha/\sqrt{2}\omega_\alpha$=Debye length for the α-th species, where $n_o=n_i=n_e$ and c is the speed of light. We also define the Alfven speed $v_A=(B^2/4\pi n_o m_i)^{1/2}$, the sound speed $c_s=((T_e+3T_i)/m_i)^{1/2}$ and the lower hybrid frequency $\omega_{LH}=\omega_i/(1+\omega_e^2/\Omega_e^2)^{1/2}$. In the analysis of the various instabilities we assume the magnetic field B is in the z direction, gradients in the densities ($\varepsilon_{n\alpha}=\nabla n_\alpha/n_\alpha$), temperatures ($\varepsilon_{T\alpha}=\nabla T_\alpha/T_\alpha$) and magnetic field ($\varepsilon_B=\nabla B/B$) lie along x and the relative electron-ion drift $\underset{\sim}{v}_d$ is along y. For shocks, the flow speed normal to the shock is V_x and the Alfven Mach number is $M_A=V_x/v_A$. For the local linear analysis we take the wavevector $\underset{\sim}{k}$ to lie in the y-z plane, $\underset{\sim}{k}=k_y y+k_z z$, with $\theta=\cos^{-1}(k_z/k)$, and assume perturbations grow as $\exp(i(\underset{\sim}{k}\cdot\underset{\sim}{x}-\omega t))$ with $\omega=\omega_r+i\gamma$.

We next recall the basic geometry of a quasiperpendicular shock, as shown in Fig. 1. (Figure and discussion is after Wu (1982).) The solid curve depicts the magnitude of the magnetic field as well as density and temperature of the various components. To the left is the upstream state with plasma flowing to the right into the shocked region; to the right is the downstream state, showing the rise in these quantities across the transition layer. According to the old idea that the shock evolves from a magnetosonic soliton due to dissipation (Tidman and Krall, Chapter 3, 1971), the width of this layer is an electron inertial length, c/ω_e. Because the width is comparable ($\beta_e\sim 1$) to an electron gyroradius, the electron orbits are significantly modified as they enter the shock. The ions, on the other hand, pass through the transition region very rapidly and are essentially unmagnetized. The difference in the electron and ion behavior leads to a charge separation, resulting in an electric field, E_x. The electrons thus experience an $\underset{\sim}{E}\times\underset{\sim}{B}$ drift across the magnetic field, which gives

rise to a cross-field current (which must be there self-consistently to provide the increase in the magnetic field dictated by Ampere's law). Besides the $\underset{\sim}{E}\times\underset{\sim}{B}$ electron drift, the gradients in the densities, temperatures and magnetic field result in additional cross-field drifts. If the shock is not perpendicular, the same arguments hold with the addition of a component of the electric field parallel to the magnetic field. For high Mach number shocks not all the ions are transmitted through the shock; rather, some are reflected at the shock front and then, depending on the geometry, return upstream or gyrate downstream.

A relative electron-ion drift can generate various plasma instabilities. These instabilities imply the growth of plasma waves which may be oscillations in the electric field alone (i.e., electrostatic fluctuations) or in the magnetic field as well (electromagnetic fluctuations). Generally, such waves grow to some level where they begin to interact back on the particles, giving rise to a frictional force that leads to plasma heating and resistivity. It is the purpose of this review to give the uninitiated reader a feeling of how this can occur as well as references where the details of the theory can be found and to give the more informed reader a summary of the present status of the field.

B. Evidence for turbulent heating

Before proceding to a detailed discussion of how to calculate plasma heating due to instabilities, we pause to ask whether such heating is really very important to shocks by considering several examples. The first example is a low Mach number, laminar quasiperpendicular shock. Figure 2 shows the evolution of various macroscopic quantities for the shock crossing of August 27, 1978 (Thomsen et al., 1984). The density and magnetic field (not shown) both increase about a factor of two across the shock. The electron temperature also increases by the same amount, consistent with compressional heating, while the ion temperature increases much more, about a factor of ten across the shock. The second example is a supercritical, nearly perpendicular shock from Nov. 7, 1977. The macroscopic quantities displayed in Fig. 3 (from Sckopke et al., 1983) again show modest increases across the shock, except for the ion temperature. In this case ion reflection provides the dissipation needed to form the shock (see reviews by Goodrich and Robson). In the downstream region, however, these reflected ions add to a very large kinetic temperature, which eventually becomes thermalized (again through an instability to be discussed later), but with a persisting non-Maxwellian shoulder.

Generally, at many of these shocks the overall electron temperature is not increased very much above its adiabatic value; however, the effect of instabilities on the electrons is not insignificant. The evolution of the electron distribution function across the transition layer for the quasiperpendicular shock of December 13, 1977 is shown in Fig. 4 (Feldman et al., 1983). In this case, which is typical of many crossings, the electron distribution becomes flattopped in the downstream region, indicating there are microscopic wave-particle interactions occurring. (See review by Feldman.)

Evidence for turbulent heating also comes from the wave measurements. Figure 5 (from Wu et al., 1984) shows the evolution of the electric field fluctuation spectrum during the shock crossing of November 7, 1977. As the spacecraft passes through the narrow transition layer, the electric noise increases by many orders of magnitude in the frequency range 100-1000 Hz. This feature is characteristic of bow shock spectra and is discussed in detail in Rodriguez and Gurnett (1975) and Gurnett's review.

C. Quasilinear transport coefficients

To show how instabilities enter into transport considerations, we derive a set of moment equations for the macroscopic quantities of interest. (For more complete discussions refer to: Davidson and Krall, 1977; Gary, 1980.) We start with the Vlasov equation for the α-th species

$$\frac{\partial f_\alpha}{\partial t} + \underset{\sim}{v}\cdot\frac{\partial f_\alpha}{\partial \underset{\sim}{x}} + \frac{e_\alpha}{m_\alpha}\left(\underset{\sim}{E} + \frac{\underset{\sim}{v}\times\underset{\sim}{B}}{c}\right)\cdot\frac{\partial f_\alpha}{\partial \underset{\sim}{v}} = 0 \qquad (1)$$

and subdivide quantities into slowly varying (on the time scale of appropriate instabilities) (denoted by $\bar{}$) and rapidly varying (denoted by $\tilde{}$)

$$f_\alpha(\underset{\sim}{x},\underset{\sim}{v},t) = \bar{f}_\alpha(\underset{\sim}{x},\underset{\sim}{v},t) + \tilde{f}_\alpha(\underset{\sim}{x},\underset{\sim}{v},t)$$

$$B(\underset{\sim}{x},\underset{\sim}{v},t) = \bar{\underset{\sim}{B}}(\underset{\sim}{x},t) + \tilde{\underset{\sim}{B}}(\underset{\sim}{x},t) \qquad (2)$$

$$\underset{\sim}{E}(\underset{\sim}{x},t) = \bar{\underset{\sim}{E}}(\underset{\sim}{x},t) + \tilde{\underset{\sim}{E}}(\underset{\sim}{x},t)$$

with $\bar{E}$ and $\bar{B}$ the equilibrium electric and magnetic fields, respectively. Upon inserting these expressions into Eq. (1) and performing an ensemble average (denoted by $\langle\rangle$), we obtain an equation for the slowly varying part of the distribution function:

$$\frac{\partial \bar{f}_\alpha}{\partial t} + \underset{\sim}{v}\cdot\frac{\partial \bar{f}_\alpha}{\partial \underset{\sim}{x}} + \frac{e_\alpha}{m_\alpha}\left(\bar{\underset{\sim}{E}} + \frac{\underset{\sim}{v}\times\bar{\underset{\sim}{B}}}{c}\right)\cdot\frac{\partial \bar{f}_\alpha}{\partial \underset{\sim}{v}} = \frac{-e_\alpha}{m_\alpha}\left\langle\left(\tilde{\underset{\sim}{E}} + \frac{\underset{\sim}{v}\times\tilde{\underset{\sim}{B}}}{c}\right)\cdot\frac{\partial \tilde{f}_\alpha}{\partial \underset{\sim}{v}}\right\rangle \qquad (3)$$

The right hand side acts as a collision term giving rise to exchange of

momentum and energy between the various plasma species and the waves. Various velocity moments can be defined:

$$\bar{n}_\alpha = \int \bar{f}_\alpha d\underset{\sim}{v}$$

$$\bar{\underset{\sim}{\Gamma}}_\alpha = \bar{n}_\alpha \bar{\underset{\sim}{V}}_\alpha = \int \bar{f}_\alpha \underset{\sim}{v} d\underset{\sim}{v} \tag{4}$$

$$\bar{\underset{\sim}{W}}_\alpha = \int \bar{f}_\alpha \underset{\sim}{vv} d\underset{\sim}{v}$$

$$\bar{Q}_\alpha = \int \bar{f}_\alpha \underset{\sim}{vvv} d\underset{\sim}{v}$$

(with similar moments for $\tilde{f}$) and moment equations can then be obtained by multiplying Eq. (3) by various components of $\underset{\sim}{v}$ and integrating:

$$\frac{\partial \bar{n}_\alpha}{\partial t} + \frac{\partial}{\partial \underset{\sim}{x}} \cdot \bar{\underset{\sim}{\Gamma}}_\alpha = 0$$

$$\frac{\partial \bar{\underset{\sim}{\Gamma}}_\alpha}{\partial t} + \frac{\partial}{\partial \underset{\sim}{x}} \cdot \bar{\underset{\sim}{W}}_\alpha + \frac{e_\alpha}{mc}(\bar{\underset{\sim}{B}} \times \bar{\underset{\sim}{\Gamma}}_\alpha) - \frac{e_\alpha}{m_\alpha} \bar{\underset{\sim}{E}} \bar{n}_\alpha = \frac{e_\alpha}{m_\alpha} \left\langle \tilde{\underset{\sim}{E}} \tilde{n}_\alpha + \frac{\tilde{\underset{\sim}{\Gamma}}_\alpha \times \tilde{\underset{\sim}{B}}}{c} \right\rangle$$

$$\frac{\partial \bar{\underset{\sim}{W}}_\alpha}{\partial t} + \frac{\partial}{\partial \underset{\sim}{x}} \cdot \bar{Q}_\alpha + \frac{e_\alpha}{m_\alpha c}(\bar{\underset{\sim}{B}} \times \bar{\underset{\sim}{W}}_\alpha) = \frac{2e_\alpha}{m_\alpha} \left\langle \tilde{\underset{\sim}{E}} \tilde{\underset{\sim}{\Gamma}}_\alpha + \frac{\tilde{\underset{\sim}{W}}_\alpha \times \tilde{\underset{\sim}{B}}}{c} \right\rangle \tag{5}$$

supplemented by Maxwell's equations:

$$\nabla \cdot \bar{\underset{\sim}{E}} = 4\pi \sum_\alpha e_\alpha \bar{n}_\alpha$$

$$\nabla \times \bar{\underset{\sim}{B}} = \frac{4\pi}{c} \sum_\alpha e_\alpha \bar{\underset{\sim}{\Gamma}}_\alpha + \frac{1}{c} \frac{\partial \bar{\underset{\sim}{E}}}{\partial t} \tag{6}$$

$$\nabla\times\bar{E} = -\frac{1}{c}\frac{\partial\bar{B}}{\partial t}$$

$$\nabla\cdot\bar{B} = 0$$

The system is a rather formidable one to solve. To see the essential features, assume a homogeneous system ($\partial/\partial x=0$), take f_α to be an isotropic Maxwellian with a net drift and sum the equation for W_α(Eq. (5)) over all three components, defining $T_\alpha=(m_\alpha/3n_\alpha)\sum_\beta W_{\beta\beta}$, to yield:

$$\frac{\partial\bar{V}_\alpha}{\partial t} + \frac{e_\alpha}{m_\alpha c}(\bar{B}\times\bar{V}_\alpha) = \frac{e_\alpha}{n_\alpha m_\alpha}\left\langle\tilde{E}\tilde{n}_\alpha + \frac{\tilde{\Gamma}_\alpha\times\tilde{B}}{c}\right\rangle$$

$$\frac{\partial T_\alpha}{\partial t} = \frac{2e_\alpha}{3n_\alpha}\langle\tilde{E}\cdot\tilde{\Gamma}_\alpha - \bar{V}_\alpha\cdot\tilde{E}\tilde{n}_\alpha\rangle \qquad (7)$$

We then define the resistivity (Davidson and Krall, 1977)

$$\nu = 4\pi\nu^*/\omega_e^2 \qquad (8)$$

in terms of the collision frequency

$$\nu^* = \frac{-e\langle\tilde{E}\tilde{n}_e + \tilde{\Gamma}_e\times\tilde{B}/c\rangle\cdot v_d}{n_e m_e v_d^2} \qquad (9)$$

and the heating frequencies

$$\nu_{T\alpha} = \frac{2e_\alpha}{3n_\alpha T_\alpha}\langle\tilde{E}\cdot\tilde{\Gamma}_\alpha - \bar{V}_\alpha\cdot\tilde{E}\tilde{n}_\alpha\rangle \qquad (10)$$

In this form it is evident that the heating and collision frequencies come from a coherent interaction of the particles with the fluctuating fields. We will show later how to evaluate such expressions.

D. Prescription for calculating dissipation

The prescription for computing the turbulent dissipation consists of the following four steps. A more detailed justification of the assumptions made in each step is found in Davidson and Krall (1977) and Gary (1980).

Step 1: Identify the instabilities. This involves first locating the sources of free energy, such as particle drifts, gradients in density, temperature, magnetic field, non-Maxwellian velocity distributions (e.g., anisotropies, loss cones, etc.). In a shock such sources may be a function of position, e.g., strong gradients and drifts in the ramp region, reflected ions in the foot, etc. (see Wu et al., 1984). Further, one has to decide on the frequency range of interest (are the ions magnetized or not) and the type of wave (electrostatic or electromagnetic) to look for.

Step 2: Solve the appropriate linear dispersion equation. In linear analysis one assumes the fluctuations grow as $\exp[i(\underset{\sim}{k}\cdot\underset{\sim}{x}-\omega t)]$ ($\omega=\omega_r+i\gamma$). (In assuming such a Fourier representation we tacitly ignore spatial dependences; hence, the calculation is a local one, at a particular position in the shock.) For electrostatic perturbations one then solves Poisson's equation, relating the perturbed electric field (expressed in terms of a potential) to the perturbed charge density:

$$\underset{\sim}{\nabla}\cdot\tilde{\underset{\sim}{E}} = i\underset{\sim}{k}\cdot(-i\underset{\sim}{k}\tilde{\phi}) = 4\pi\Sigma_\alpha e_\alpha\tilde{n}_\alpha \quad . \tag{11}$$

Since (as shown below) n_α can be related to ϕ

$$\tilde{n}_\alpha = \chi_\alpha\tilde{\phi} \tag{12}$$

one obtains

$$k^2\tilde{\phi} = 4\pi\,\Sigma_\alpha e_\alpha\chi_\alpha\tilde{\phi} \quad , \tag{13}$$

or a dispersion equation

$$k^2 - 4\pi\Sigma_\alpha e_\alpha\chi_\alpha = 0 \tag{14}$$

relating ω and k with properties of the plasma.

The perturbed charge density is obtained by integrating the perturbed distribution $\tilde{f}_\alpha$ over velocity (Eq. (4)). $\tilde{f}_\alpha$ is obtained from the linearized Vlasov equation:

$$\frac{\partial \tilde{f}_\alpha}{\partial t} + \underset{\sim}{v}\cdot\frac{\partial \tilde{f}_\alpha}{\partial \underset{\sim}{x}} + \frac{e_\alpha}{m_\alpha}\left(\tilde{\underset{\sim}{E}} + \frac{\underset{\sim}{v}\times\tilde{\underset{\sim}{B}}}{c}\right)\cdot\frac{\partial \tilde{f}_\alpha}{\partial \underset{\sim}{v}} = 0 \tag{15}$$

which can be solved by the method of characteristics (Krall and Trivelpiece, Chapter 8, 1973)

$$\tilde{f}_\alpha = \frac{e_\alpha}{m_\alpha}\int dt' \exp\{i\underset{\sim}{k}\cdot(\underset{\sim}{x}'-\underset{\sim}{x})-\omega(t'-t)\}\left(\tilde{\underset{\sim}{E}} + \frac{\underset{\sim}{v}'\times\tilde{\underset{\sim}{B}}}{c}\right)\cdot\frac{\partial \bar{f}_\alpha}{\partial \underset{\sim}{v}'} \tag{16}$$

along the orbit $\underset{\sim}{x}'(t')$, $\underset{\sim}{v}'(t')$ such that $\underset{\sim}{x}'(t)=\underset{\sim}{x}$ and $\underset{\sim}{v}'(t)=\underset{\sim}{v}$. In general, this can be a complicated business, especially when gradients are included.

For electromagnetic perturbations the same procedure is followed, except now one solves the other Maxwell's equations as well:

$$\nabla\times\tilde{\underset{\sim}{E}} = -\frac{1}{c}\frac{\partial \tilde{\underset{\sim}{B}}}{\partial t}$$

$$\nabla\times\tilde{\underset{\sim}{B}} = \frac{4\pi}{c}\tilde{\underset{\sim}{j}} + \frac{1}{c}\frac{\partial \tilde{\underset{\sim}{E}}}{\partial t} \tag{17}$$

$$\nabla\cdot\tilde{\underset{\sim}{B}} = 0$$

where

$$\tilde{\underset{\sim}{j}} = \Sigma e_\alpha \tilde{\underset{\sim}{\Gamma}}_\alpha = \sigma\cdot\tilde{\underset{\sim}{E}}. \tag{18}$$

These equations reduce to:

$$\underset{\sim}{k}\times(\underset{\sim}{k}\times\tilde{\underset{\sim}{E}}) + \frac{\omega^2}{c^2}\tilde{\underset{\sim}{E}} + \frac{4\pi i\omega}{c^2}\sigma\cdot\tilde{\underset{\sim}{E}} = D\cdot\tilde{\underset{\sim}{E}} \qquad (19)$$

and thus the dispersion equation is

$$\text{Det } |D| = 0. \qquad (20)$$

In addition to being necessary for computing the dissipation, the linear analysis reveals under what conditions the instability exists ($\gamma>0$) and how its characteristics vary with the parameters of the system. Indeed, most of the work on instability theory for shocks (as well as elsewhere) is concerned with such local, linear analysis.

Step 3: Estimate the fluctuation level. In the evaluation of the resistivity or the heating rates (Eqs.(8-10)), quantities like $\langle\tilde{\underset{\sim}{E}}\cdot\tilde{\underset{\sim}{\Gamma}}_\alpha\rangle$ and $\langle\tilde{\underset{\sim}{E}}\tilde{n}_\alpha\rangle$ have to be evaluated. From linear theory relations between $\tilde{\underset{\sim}{\Gamma}}_\alpha$ or n_α and $\underset{\sim}{E}$ can be obtained (Eqs. (12) and (18)) and the ensemble averages can then be evaluated

$$\langle\tilde{E}_i\tilde{n}_\alpha\rangle = \langle\Sigma_j\tilde{E}_i\chi_\alpha\tilde{E}_j\rangle = \langle\Sigma_j(\Sigma_{k,\omega}\tilde{E}_i(k,\omega))(\Sigma_{k,\omega}\tilde{E}_j(k',\omega')\chi_\alpha(k',\omega'))\rangle \qquad (21)$$

The ensemble averages imply that only waves in phase contribute (i.e., Random Phase Approximation),

$$\langle\tilde{E}_i\tilde{n}_\alpha\rangle = \Sigma_{k,\omega}|E_i(k,\omega)|^2\chi_\alpha(k,\omega) \quad . \qquad (22)$$

The quantity, $|\underset{\sim}{E}(k,\omega)|/8\pi=\varepsilon_k$, is the energy density in one particular mode. According to linear theory, if an instability exists, the unstable waves grow exponentially; but growth eventually ceases at some finite level and the task is to determine ε_k when this occurs. There are various ways to do this, which may vary from instability to instability, some of which will be described in the next section.

One rather easy method to get an upper bound on the fluctuation level which is commonly used is to assume that all of the free energy is converted to fluctuations. This often gives the correct scaling of the saturation level with macroscopic parameters, although it can overestimate the fluctuation level by quite a bit, depending on how much of the free energy goes into heating of the plasma instead and how much free energy remains when the instability is stabilized. The procedure is usually simplified further by assuming all the wave energy resides in one mode, typically the one most unstable according to linear theory. It should be pointed out, however, that this method

does not necessarily work well for the shock, where a stationary state is reached by balancing the rate of growth of the instability with the rate of dissipation, rather than by relaxing the free energy to achieve a marginally stable state.

A common alternative method for obtaining the fluctuation level is to run some sort of computer simulation of the instability. This is a very useful technique, which allows at the same time the opportunity to verify linear theory and measure heating rates as well. Again, the boundary conditions which are often imposed to study the instabilities in idealized situations are not always appropriate to conditions in the shock. Such simulations are valuable nevertheless, and some examples will be given in the next section. Interested readers are urged to read Vols. 9 and 16 of Methods of Computational Physics (Academic Press) and the forthcoming book on simulation methods for space plasmas by H. Matsumoto and T. Sato (D. Reidel, 1984).

Step 4: Solve the transport equations. Generally, the full set of equations (5-6) is too difficult to solve and so approximations to reduce them to just expressions for the heating rates and resistivity (8-10) are made. Even in this simplified form the results are useful and expressions for the various instabilities have been collected together. For example, Liewer and Krall (1973) have obtained expressions for the instabilities relevant to perpendicular shocks. Lampe et al. (1975) have a more inclusive set for hydrodynamic instabilities. Davidson and Krall (1977) have collected the transport coefficients needed to model theta-pinch experiments. Gary (1980) has put together a complete formalism for electrostatic, cross-field instabilities, whose nonlinear behavior has been treated in a consistent fashion. Transport coefficients can be derived in a much more elegant manner as well (Dum, 1978a and 1978b), as will be shown later.

It is also possible to solve the time-dependent transport equations numerically, with the anomalous terms evaluated locally in space and time (e.g., see Davidson and Krall (1977) and review by Papadopoulos, this meeting). This technique has been successfully employed in analyzing theta-pinch experiments (Hamasaki et al., 1977), although the level of agreement between calculation and experimental measurements is no better than when simplified phenomenological expressions for the transport coefficients (Sgro, 1978) are used. Such calculations are generally complicated and to extend them to oblique geometries becomes even more of a problem because the nonlinear character of the various cross-field instabilities is then somewhat uncertain and other dissipation processes come into play.

III. Instabilities

We now use the prescription described in the previous section to investigate the instabilities responsible for dissipation in collisionless shocks. After identifying which modes are thought to be the most important we examine each in turn and summarize the current knowledge about their linear, nonlinear, and transport properties, particularly in regard to shocks.

A. Classification

To identify the instabilities we refer back to Fig. 1 to recall the sources of free energy. For quasiperpendicular shocks the principal source of free energy is the cross-field current, i.e., the

relative electron-ion drift across the magnetic field due to the $\underline{E}\times\underline{B}$ drift, the ∇B drift, and diamagnetic drifts due to density and temperature gradients. There can also be relative electron-ion drifts along the magnetic field. Furthermore, the conservation of the magnetic moment of the electrons and increase of the magnetic field at the shock produces a temperature anisotropy, $T_{e\perp}/T_{e\parallel} > 1$. For supercritical shocks ion reflection occurs, which leads to relative electron-ion drifts in the foot region and a large energy anisotropy, $E_\perp/E_\parallel$, downstream of the main shock transition. The reflection process generates a large amount of free energy in the reflected ion component that can have a very significant effect on the various microinstabilities at the shock, as emphasized by Wu et al. (1984).

Following the observations (Rodriguez and Gurnett, 1975 and 1976; Wu et al., 1984; Gurnett review this meeting), we subdivide the instabilities into high frequency waves that are electrostatic and low frequency modes which have a strong electromagnetic component. The high frequency modes to be discussed include the ion acoustic instability (with a little about the hydrodynamic limit--the Buneman instability--included) and the electron cyclotron drift instability. The low frequency modes include the ion-ion instability, the modified two stream (also known as the kinetic cross-field streaming) instability, and the lower hybrid drift instability. For the most part we consider each of these modes as isolated cases; few papers compare the various instabilities under similar conditions, especially for shocks. There are two notable exceptions (Lashmore-Davies and Martin, 1973; Lemons and Gary, 1978), which provide valuable insight to the interconnection of the various modes.

There are, of course, many other instabilities as well. Waves at or below the ion cyclotron frequency (including most drift waves) are generally ignored, because the time scales for these waves to transverse the shock is too short for them to grow to appreciable levels. Other modes which could contribute will be discussed only very briefly, either because they have been treated in only a limited manner (e.g., ion velocity ring modes, Wu et al., 1984), or they are being considered in other reviews at this meeting (e.g., parametric decay instabilities at quasiparallel shocks by Quest, beam-like ion acoustic modes by Feldman, electron whistlers by Gurnett, and the electromagnetic ion cyclotron instability which thermalizes reflected ions by Goodrich).

B. High frequency instabilities

1. Ion acoustic instability

The ion acoustic instability has been the most often invoked process for explaining turbulent heating and resistivity in shocks. Its linear properties are well known (e.g., Krall and Trivelpiece, Chapter 8, 1973). The ion acoustic instability is an electrostatic mode driven by relative electron-ion drifts along or across a magnetic field. The instability is driven by a resonant interaction with the electrons $[(\omega-kv_d)/k_\parallel v_e \ll 1]$ while the ions are nonresonant $(\omega/kv_i \gg 1)$. More importantly, there is a threshold condition for instability, $v_d > c_s$. When $T_i = T_e$ the threshold is very high, $v_d > v_e$, and the instability becomes fluid-like rather than kinetic and is usually referred to in this limit as the Buneman instability. (Because the threshold is so high, implying a current layer thickness $< c/\omega_e$ $(\beta_e \approx 1)$, it is less interesting for shock applications.) In the case of a

cross-field current (with $\underset{\sim}{j}$ along y and $\underset{\sim}{B}$ along z) for $\underset{\sim}{k}$ not parallel to $\underset{\sim}{j}$ (i.e., $\underset{\sim}{k}=k_y y+k_z z$) the linear dispersion equation reduces to that of the (B=0) ion acoustic mode. As k_z goes to zero, the resonant nature of the electrons is lost and the instability goes over to the electron cyclotron drift instability, to be discussed later.

The linear properties of the ion acoustic mode are given by (for maximum growth):

$$\omega_r = kc_s(1 + k^2\lambda_{De}^2)^{-1/2} \tag{23}$$

$$\gamma = (\frac{\pi}{8})^{1/2}\frac{|\omega_r|}{(1 + k^2\lambda_{De}^2)^{3/2}} \quad (\frac{m_e}{m_i})^{1/2}(\frac{\underset{\sim}{k}\cdot\underset{\sim}{v}_d}{\omega_r}-1) - (\frac{T_e}{T_i})^{3/2}\exp[\frac{-T_e}{2T_i(1 + k^2\lambda_{DE}^2)}]$$

or in the limit $v_e>v_d>>c_s$

$$\omega_r = \omega_i/\sqrt{3}$$

$$k = (2\lambda_{De})^{-1/2} \tag{24}$$

$$\gamma = \frac{1}{3}(\frac{\pi m_e}{6m_i})^{1/2}\frac{v_d}{c_s}\omega_i \quad ,$$

while those of the Buneman instability are:

$$\omega_r = \frac{1}{2}(\frac{m_e}{2m_i})^{1/3}\omega_e$$

$$\gamma = \sqrt{3}\,\omega_r \tag{25}$$

$$k = \omega_e/v_d \quad .$$

For shock geometries the threshold condition for the ion acoustic instability (which is roughly $(v_d/v_e)(T_e/T_i)>1$) can be reduced by

gradients in the density and electron temperature (Priest and Sanderson, 1972; Soldner et al., 1977). The gradients distort the electron distribution function, increasing its derivative at $v=\omega/k$. In high Mach number quasiperpendicular shocks distortions in the ion distribution function caused by the presence of reflected ions can similarly lower the threshold for the instability by reducing the ion Landau damping (Wu et al., 1984).

The understanding of the nonlinear behavior of the ion acoustic instability has not advanced much in recent years, so that Papadopoulos (1977) remains an excellent summary. In the case of a cross-field current the magnetic field prevents electron runaway and keeps the electron velocity distribution isotropic. Saturation of the instability is then due to nonlinear ion dynamics, which have been described in several ways. In the weak turbulence approach (Kadomsev, 1965; Sagdeev and Galeev, 1969) linear growth is balanced by nonlinear Landau damping to give a saturation level

$$W = \frac{|\tilde{E}|^2}{8\pi n T_e} \approx 10^{-2} \frac{v_d}{v_e} \frac{T_e}{T_i} \quad , \tag{26}$$

a spectrum for the fluctuations

$$|\tilde{\phi}|^2 \sim \frac{1}{k^3} \ln \frac{1}{k\lambda_{De}} \quad , \tag{27}$$

a collision frequency

$$\nu^* \approx 10^{-2} \frac{T_e}{T_i} \frac{v_d}{v_e} \omega_e \quad , \tag{28}$$

and a sheath width

$$\Delta \sim 10^{-1} \left(\frac{\omega_e}{\Omega_e}\right)^{1/3} \left(\frac{m_i}{m_e}\right)^{1/3} \beta_e^{-2/3} \, c/\omega_e \quad . \tag{29}$$

Galeev (1976) gives another derivation, finding

$$\Delta \sim \left(\frac{m_e}{m_i}\right)^{1/4} \beta_e^{-1/2} \left(M_A^2 - 1\right) \; c/\omega_i \quad . \tag{30}$$

Horton et al. (1976) have redone the weak turbulence theory more carefully (removing some of the numerical divergences) and solved the resulting time-dependent mode coupling equations for the turbulent spectrum. Scaling laws based on this renormalized theory have also been obtained (Horton et al., 1979).

In another approach (Sleeper et al, 1973; Wesson and Sykes, 1973) the linear growth of the waves is balanced by a broadening of the ion Landau resonance due to the perturbation of the ion orbits by the turbulence. The result is a complicated set of equations for the angular spectrum which can be solved numerically. A third approach (Tystovich, 1972) is based on a kinetic wave equation which includes a nonlinear broadening of the decay condition.

The nonlinear theories also give values for the resistivity (e.g., weak turbulence result above). Gary (1980) has computed the resistivity and heating rates assuming the saturation level is determined by ion trapping (Biskamp and Chodura, 1971). Dum (1978a) has derived the transport coefficients for the ion acoustic instability in a more elegant fashion, by considering a kinetic equation which includes collisions due to Coulomb interactions as well as turbulence. The electron distribution, derived self-consistently, is flattopped (e.g., Fig. 4), $f_e \sim \exp[-(|v|/v_e)^{-s}]$ ($s \sim 4$-6). The transport consistent with this distribution (resistivity and heating) is significantly modified from that obtained with a simple Maxwellian ($s=2$) distribution. In a second paper (Dum, 1978b) the theory is extended to include gradients and a parallel current.

The nonlinear theories have been supported by simulation studies (Morse and Nielson, 1971; Biskamp and Chodura, 1971), the most realistic of which are the two-dimensional calculations of Dum et al. (1974) with a current (that was kept constant) across a weak magnetic field. Instead of forming a stationary state, the fluctuations grow, saturate, and then relax, eventually returning to near thermal levels. The electrons are slightly heated and form a flattopped distribution, while high energy ion "tails" are formed, instead of bulk ion heating.

The ion acoustic instability is almost always proposed to explain the observed electrostatic waves at the bow shock (Rodriguez and Gurnett, 1975 and 1976), although there have been no direct measurements of the wavelengths and little theoretical analysis. Evidence for its existence enters indirectly, by the observation of flattopped electron distributions (Feldman et al., 1983) and through the use of a marginal stability condition to explain the width of quasiperpendicular, laminar shocks (Morse and Greenstadt, 1976; Greenstadt et al., 1978). The shock widthth, Δ, is determined from Ampere's law with the value of the current such that the ion acoustic instability relaxes to its marginal stability condition, $v_d^* = c_s f(T_e/T_i)$ (Manheimer and Boris, 1972):

$$\Delta = \frac{\Delta B}{B} \frac{1}{\beta_e^{1/2}} \frac{1}{\xi} \frac{c}{\omega_i} \quad . \tag{31}$$

On the other hand, more recent data from ISEE-1 and 2 (Russell et al, 1982) suggest that the shock width is better fit by the weak turbulence condition (30), or simply c/ω_i, rather than the marginal stability condition. However, Russell et al. do not explain how the shocks they observe can be too broad to satisfy the ion acoustic condition, yet be well described by a theory based on ion acoutic turbulence.

For the ion acoustic instability to be effective, and not require steep gradients, $T_e/T_i \gg 1$ is needed. This condition is not always met, however. In some cases (see Biskamp, 1973) there are suggestions that the leading edge of the shock can steepen up so that $v_d > v_e$, triggering the Buneman instability. When this occurs, the electrons are strongly heated, as seen in both simulations in both one (Morse and Nielson, 1971; Davidson et al., 1971) and two (Lampe et al, 1974; Dum and Chodura, 1979) dimensions, so that the usual ion acoustic instability can then operate throughout the rest of the shock. This preheating does not always occur (e.g., the bow shock); sometimes $T_e/T_i < 1$ persists and another instability mechanism, the electron cyclotron drift instability, is needed.

2. Electron cyclotron drift instability

This instability exists in a small region of k-space near $k_z = 0$ (for $\underline{j}$ along y and B along z) and results from the coupling of a Doppler shifted Bernstein wave and an ion wave. (See Lashmore-Davies and Martin, 1973).) For $T_e/T_i \gg 1$, it is a fluid instability and becomes ion-acoustic-like for $k_z \neq 0$. Its domain of instability (k_z/k) increases with v_d/v_e. Most importantly, the instability persists for $T_e/T_i < 1$, becoming kinetic in nature. For $k_y \rho_e \gg 1$, its linear properties are given by (Lashmore-Davies and Martin, 1973)

$$\omega_r = k_y v_d - n\Omega_e$$

$$\gamma = \Omega_e \frac{n^{1/2}}{(8\pi)^{1/4}} \left(\frac{m_e}{m_i}\right)^{1/4} (1 + k^2 \lambda_{De}^2)^{-3/4} \tag{32}$$

$$k_y v_d = n\Omega_e + k c_s (1 + k^2 \lambda_{De}^2)^{-3/4} \quad .$$

The existence of this mode for shocks has been debated. Equation (32) suggests it would be found in (Doppler shifted) bands around Ω_e. (Note that because $\omega_e \gg \Omega_e$ at the shock, $\Omega_e \sim \omega_i$, so that is difficult to distinguish this mode from the ion acoustic.) Wu and Fredricks (1972) argue that the narrow band spikes of electrostatic noise observed by OGO-5 were signatures of the instability, although such features were

not found in more recent IMP-6 (Rodriguez and Gurnett, 1975) and ISEE data (Greenstadt et al., 1980). It has been recently shown by Zhou et al. (1984) that magnetic field gradients stabilize the instability for perpendicular shocks, perhaps suggesting why it is not often observed.

Another reason why it is not usually seen may be because the instability saturates at low levels (Lampe et al., 1972a). Since the instability involves undamped Berstein waves, any perturbation of the electron orbits is a stabilizing effect. Based on this idea, it is easy to estimate the saturation level assuming the limiting level of turbulence is such that a particle diffuses half a wavelength in one gyroperiod (Biskamp and Chodura, 1973):

$$D \simeq \frac{(\Delta x)^2}{\Delta t} \simeq \frac{1}{2}\,\pi\,\frac{\Omega_e}{k^2} \quad . \tag{33}$$

Using a simple Fokker-Planck diffusion model, D can be approximated as

$$D = (2\pi)^{1/2}\,\frac{\omega_e^2}{\Omega_e^2}\,\frac{|\tilde{E}|^2}{8\pi n T_e}\,\frac{v_e}{\langle k\rangle} \quad . \tag{34}$$

Combining these two results yields the saturation level:

$$W = \frac{|\tilde{E}|^2}{8\pi n T_e} = \left(\frac{\pi}{8}\right)^{1/2}\,\frac{\Omega_e^2}{\omega_e^2}\,\frac{\Omega_e}{k v_e}\,\frac{\langle k\rangle}{k} \quad . \tag{35}$$

Since $kv_e \sim \omega_e$ and $\omega_e >> \Omega_e$, W is very small. That would be the end of the story, except that computer simulations (which originally showed the potency of the instability (Forslund et al., 1970)) revealed that a nonlinear electron cyclotron instability is also excited (Forslund et al., 1971; Lampe et al., 1971; Biskamp and Chodura, 1972). This nonlinear instability cannot be described by a dispersion equation and one has to rely on computer simulation for insight.

The nonlinear evolution of the instability in part depends on how the simulations are conducted. In one-dimensional calculations the instability strongly heats electrons and ions and suggests a coherent process occurs. In this case the heating rate $v_e^{\cdot} \simeq$ constant and phase space pictures indicate that the electrons continuously become trapped and then untrapped by the magnetic field. When v_e increases so that v_d (kept constant) $\simeq v_e(\Omega_e/\omega_e)$ the instability switches off. The condition

for starting the instability looks very much like the ion acoustic condition ($(v_d/v_e)(T_e/T_i)>1/2$) (Lampe et al, 1972b), but this can be reduced by the presence of turbulence (Biskamp and Chodura, 1973). In two dimensions the instability is much weaker and the electron heating is more stochastic. It has been studied only in the case $T_e>>T_i$, where it looks like the unmagnetized ion acoustic instability.

Finally, it should be mentioned that in high Mach number quasiperpendicular shocks reflected ions can also drive the electron cyclotron drift instability (linearly) in the direction of the shock normal. This has been observed in a theta-pinch experiment (Gold et al., 1980) and may explain some of the high frequency noise observed at the shock. Whether it has (or is) a nonlinear analogue is not known at present.

C. Low frequency instabilities

1. Ion-ion instability

Like the electron cyclotron drift instability the ion-ion instability was investigated extensively a decade ago and little has been done since. An excellent discussion of its properties is found in Biskamp (1973). The linear theory is derived most simply in the case of two equal density beams, counterstreaming ($\pm v_d$) perpendicular to the magnetic field. Assuming strongly magnetized electrons ($\omega<<\Omega_e$) and unmagnetized ions ($\omega>>\Omega_i$) the maximum growth rate and corresponding wavenumber are (Papadopoulos et al., 1971):

$$\gamma = \omega_{LH}/\sqrt{8}$$

$$k = \sqrt{3}\gamma/v_d \quad .(36)$$

For unequal beams the dispersion equation has to be solved numerically; ω_r and γ lie in the lower hybrid frequency range. For finite β_e the instability stabilizes when

$$v_d \cos\alpha \lesssim v_A(1+\beta_e)^{1/2} \quad , \qquad (37)$$

where $\underset{\sim}{k}\cdot\underset{\sim}{v}_d = kv_d\cos\alpha$. For modes propagating parallel to the beam direction then stability occurs when the beam speed is roughly the Alfven speed; the condition (37), however, states that for any v_d, there will always be some off-angle modes which are unstable (with somewhat smaller growth rates). Kinetic corrections to the linear dispersion equation have been discussed by Auer et al. (1971) and recently reexamined by Wu et al. (1984). These calculations show, for example, that for fixed β_i, the instability is enhanced by increasing β_e.

One-dimensional simulations (Papadopoulos et al, 1971) demonstrate that the instability leads to strong ion heating (trapping) for $v_d<v_A$ and the heating process can be described by a set of quasilinear rate equations. Later calculations verified that finite beta stabilization occurs for $v_d>v_A$ (Wagner et al., 1971). This has been shown more clearly in recent two-dimensional calculations by Lee et al. (1981). In cases where the parallel (cos α=1) modes are stable, the oblique modes still grow, but no strong ion heating occurs.

It was originally thought that the ion-ion instability would occur between the solar wind ions and the reflected ions in supercritical quasiperpendicular shocks, leading to the observed strong ion heating (Auer et al, 1971; Papadopoulos, 1971). Generally the velocity difference between the two streams is much larger than the Alfven speed and the instability is stabilized. There is no evidence from spacecraft observations (e.g., Fig. 3) or from simulation (Liewer, 1976; Leroy et al., 1982; Forslund et al., 1984) that it does occur. In simulations of oblique shocks, however, Biskamp and Welter (1972) observed a strong ion-ion interaction, which they attributed to the ion-ion instability, excited nonlinearly by potential fluctuations due to whistler waves. Forslund et al. (1972) have attributed the same phenomena to a whistler decay instability. This behavior has not been seen in recent simulations of oblique shocks (Quest et al., 1983; Leroy and Winske, 1983), perhaps because of numerical constraints in the models. (See review by Quest for details.)

Although reflected ions do not seem to excite the ion-ion instability, they can interact with the electrons to produce unstable waves, as shown next.

2. Modified-two-stream instability

The modified two stream instability is another well known instability of the early Seventies (Krall and Liewer, 1971). For β=0, it is an electrostatic mode that results from the coupling of a lower hybrid wave and a Doppler shifted electron plasma oscillation (Lashmore-Davies and Martin, 1973). For the usual case of electrons drifting relative to ions along y across a homogeneous magnetic field Bz, the instability propagates almost in the y direction (cos $\theta \approx (m_e/m_i)^{1/2}$). Because the electrons are strongly tied to the magnetic field, this constraining motion gives them an effective mass and the instability is a hydrodynamic mode involving the relative streaming of the heavy ions and the effectively equally heavy electrons (from which the name "modified two stream" derives). At maximum growth the properties of the most unstable mode are:(McBride et al , 1972)

$$\omega_r = \frac{\sqrt{3}}{2}\,\omega_{LH}$$

$$\gamma = \frac{1}{2}\,\omega_{LH} \qquad (38)$$

$$k \simeq \sqrt{3}\,\frac{\omega_{LH}}{v_d} \quad .$$

For large value of k_z/k the instability goes over to the ion acoustic mode (which is damped for $T_i \simeq T_e$). The modified two stream instability persists for $T_i > T_e$, but is stabilized by electromagnetic effects when the drift speed exceeds the Alfven speed (McBride and Ott, 1972).

An interesting feature of this instability is that it heats both electrons and ions: the ions are heated primarily in the direction of the current, while the electron heating is along the magnetic field. This has been verified in two-dimensional particle simulations (McBride et al., 1972), that show the nonlinear behavior is due to the fact that both electrons and ions become trapped (the unmagnetized ions are trapped by the fluctuating electric field along k, while the electrons are trapped by the $E_\parallel$ component). The amount of heating that could occur at the bow shock from this instability has been estimated by Revathy and Lakina (197

As with the ion-ion instability the aforementioned electromagnetic stabilization that occurs for $v_d > v_A$ would seem to preclude the possibility of it being an effective heating mechanism at the bow shock. The effect of finite beta on the instability, however, is quite interesting and has been investigated extensively over the last few years (Lemons and Gary, 1977; Wu et al., 1983; Wu et al., 1984; Tsai et al., 1984), particularly with application to supercritical shocks. In this case the reflected ions just in front of the shock (in the 'foot') are streaming relative to the incoming solar wind ions (too fast to excite the ion-ion instability). In the shock normal (x) direction these two ion species are drifting relative to the electrons across the magnetic field, allowing for the possibility of exciting electron-ion instabilities with each ion component.

When $\beta \sim 1$, the dispersion equation is very complicated and there are no simple analytic expressions. Compared to the $\beta = 0$ result, the growth rate is reduced (but still a sizeable fraction of ω_{LH}), $k \sim \omega_e/c$, and the angle of propagation θ is more oblique. An example of such linear results (from Tsai et al, 1984) is shown in Fig. 6. As v_d is increased beyond v_A, the instability is not stabilized, rather θ decreases while the corresponding maximum growth rate increases up to $v_d/v_A \sim 10$ then decreases. The instability in this regime results from the coupling of the ion beam with whistler modes (Wu et al, 1983), the hydrodynamic character of the modified two stream instability is lost, and the mode is more appropriately termed "the kinetic cross-field streaming instability".

An interesting property of this instability was found by Lemons and Gary (1977). They showed that the magnetic part of the instability $|B|^2$ can be large compared to the electric part $|E|^2$, even though the instability is primarily electrostatic in origin. This follows by separating the electric field into its longitudinal and transverse components ($\underline{E} = \underline{E}_L + \underline{E}_T$) and recalling that

$$\nabla \times \underline{E}_T = \frac{-1}{c} \frac{\partial B}{\partial t} \quad . \tag{39}$$

Since $|\omega/ck|^2 \ll 1$, $|B|^2/|E|^2$ can be large even though $|E_T|^2/|E_L|^2 \ll 1$. At the bow shock the low frequency electromagnetic noise has often been attributed to whistlers (Rodriguez and Gurnett, 1975 and 1976); the above arguments suggest that much of this low frequency (<100Hz) noise can be due to modes like the kinetic cross-field streaming instability.

Heating at the bow shock due to this instability at high beta has also been investigated. Winske et al. (1984) have worked out a quasilinear theory for the heating parallel and perpendicular to B for arbitrary β. As β increases and the most unstable mode propagates more obliquely, the electron and ion heating become more isotropic. To calculate the actual heating rates the saturation level for the instability is needed. Computer simulations (Winske et al., 1984) demonstrate that the saturation level decreases with β; this occurs because as beta increases and the most unstable modes propagate more in the direction of the magnetic field, it becomes easier to trap the electrons. The heating rates decrease with beta as well, as shown in Fig. 7. These results have been applied to heating at the bow shock, assuming unstable waves are generated both from the presence of reflected and solar wind ions in the foot region. For low β, waves due to both species effectively heat the electrons, increasing their parallel temperature across the shock by about a factor 5-10. At $\beta=1$, however, only waves due to the solar wind ions heat the electrons, but much less effectively, $\Delta T_e/T_e \sim 40\%$.

In the ramp region the effect of gradients (∇n, ∇T) are also important, and the kinetic cross-field instability acquires a somewhat different character and a new name, the lower hybrid drift instability.

3. Lower hybrid drift instability

When $k_z=0$ the kinetic cross-field streaming instability is stable. The presence of gradients in density and temperature destabilizes the mode and it is then called the lower hybrid drift instability. The distinction between the two instabilities is partly historical and derives from the response of the electrons. In the case of the kinetic cross-field streaming instability, the electrons are free to move along the magnetic field, while for the lower hybrid drift instability they are strongly constrained because $k_z=0$. Actually the two instabilities are limiting cases of the same entity. In a self-consistent equilibrium the cross-field current which would give rise to the kinetic cross-field streaming instability would be due to gradients and in a three-dimensional system waves with $k_z=0$ would form a small subset of the entire spectrum. Thus, the two modes can be combined into a 'generalized lower hybrid drift instability' (Hsia et al., 1979).

The lower hybrid drift instability has been extensively studied with applications to theta-pinch experiments and the earth's magnetotail (Krall and Liewer, 1971; Davidson and Gladd, 1975; Coppi, 1976; Davidson et al., 1977; Huba et al, 1981) In such situations the plasma pressure is balanced by the magnetic pressure, so that the density gradient and the magnetic field gradient are in opposite directions. (This is not so at the shock, as will be discussed later.) The instability is fluid-like for $v_d=|v_{ne}+v_{ni}|>v_i$ with linear properties (for $v_d/v_i \gg 1$ and $T_e/T_i \ll 1$):

$$\omega_r = \frac{1}{2^{5/6}} \left(\frac{v_{di}}{v_i}\right)^{1/3} \omega_{LH}$$

$$\gamma = \sqrt{3}\, \omega_r \qquad (40)$$

$$k = \sqrt{2}\, \frac{\omega_{LH}}{v_i}$$

and kinetic for $v_d/v_i<1$ with characteristics (for $v_d/v_i<<1$):

$$\omega_r = \frac{1}{\sqrt{2}} \frac{v_{di}}{v_i} \omega_{LH}$$

$$\gamma = \frac{(2\pi)^{1/2}}{8} \left(\frac{v_{di}}{v_i}\right)^2 \omega_{LH} \qquad (41)$$

$$k = \sqrt{2}\, \frac{\omega_{LH}}{v_i}$$

The instability is rather insensitive to T_e/T_i, but enhanced by $T_e/T_i<1$, and does not become stabilized when the drift speed v_d is lowered. (For $v_d<<v_i$, it evolves into an ion cyclotron mode (Freidberg and Gerwin, 1977).)

The heating rates and collision frequency for the lower hybrid drift instability have been calculated by Davidson and Gladd (1975) and Gary (1980), who finds ($T_e/T_i<<1$):

$$\nu^* = \frac{(2\pi)^{1/2}}{10} \left(\frac{T_i}{T_e}\right)^{5/4} \left(\frac{v_{di}}{v_i}\right)^2 \omega_{LH}$$

$$\nu_{Ti} = \frac{(2\pi)^{1/2}}{15} \left(\frac{T_i}{T_e}\right)^{1/4} \left(\frac{V_{di}}{v_i}\right)^4 \frac{m_e}{m_i} \omega_{LH} \qquad (42)$$

$$\nu_{Te} = \frac{1}{(10)^{1/2}} \left(\frac{T_i}{T_e}\right)^{5/4} \nu_{Ti} \quad .$$

The instability heats electrons as well as ions. These results have been verified in a number of computer simulations (e.g., Winske and Liewer, 1978; Tanaka and Sato, 1981; Chen et al., 1983 Brackbill et al., 1984).

The nonlinear turbulence level of the instability was initially estimated from the available free energy (Davidson and Gladd, 1975). More recently, computer simulations (again in theta-pinch or neutral sheet geometry, mostly in two dimensions) have been used to calculate the saturation level and to try to determine whether the electrons or the ions are the ultimate dissipative mechanism (see Winske, 1981). Early simulations considered stronger (fluid-like) cases ($v_d >> v_i$) and ion trapping was clearly demonstrated to be the saturation mechanism (Winske and Liewer, 1978; Tanaka and Sato, 1981). In weaker cases ($v_d \approx v_i$) the saturation process was unclear. In the last few years, however, other simulations of the kinetic regime ($v_d < v_i$) (Chen et al., 1983; Brackbill et al., 1984) have now, with some confidence but not conclusively, shown that the electrons provide the ultimate dissipation through ∇B resonance effects, consistent with recent nonlinear theory (Drake et al., 1983 and 1984).

In the shock geometry the situation is somewhat different, because the density gradient and magnetic field gradient are in the same direction. In this case the usual lower hybrid drift mode is stable (Lemons and Gary, 1978), although it can be destabilized by an electron temperature gradient (Zhou et al., 1983). This is shown in Fig. 8, from Zhou et al; for $\epsilon_T \rho_i < 1$ the mode is stable at $\theta = 90^\circ$, while for larger values of $\epsilon_T \rho_i$ the instability peaks at $\theta = 90^\circ$.

Recent two-dimensional simulations of quasiperpendicular shocks (Forslund et al., 1984) show heating of transmitted ions, in addition to the appearance of reflected ions. Figure 9 presents a snapshot of one of the simulations, showing phase space and the magnetic field structure along the shock normal and wave activity inside the shock layer. The wavelengths and frequencies of the strong fluctuations that are observed in the calculation are typically c/ω_e and ω_{LH}, respectively. An analysis of these waves (Fig. 9d) using profiles obtained from the simulation (Aldrich et al., 1983) has shown that the frequencies and wavelengths are consistent with the lower hybrid drift instability (with $k_z \neq 0$) of Zhou et al. (1983). Waves are also observed in the foot region (Fig. 9c), where the gradients are not predominant (Fig. 9b) but the reflected ions form a distinct population (Fig. 9a). The waves here can be attributed to the interaction of both ion components with the elecrons via the kinetic cross-field streaming instability (Wu et al., 1984). These lower hybrid-like waves in the simulation are consistent with the low

frequency electromagnetic waves usually observed at bow shock crossings (Rodriguez and Gurnett, 1975 and 1976).

Finally, we conclude this subsection with an important point, made by Lemons and Gary (1978). Although the lower hybrid drift and kinetic cross-field streaming instability have much lower thresholds than the ion acoustic instability, the shock width is better fit by a condition based on the marginal stability velocity of the ion acoustic instability (Morse and Greenstadt, 1976; Greenstadt et al., 1978). The reason is that the anomalous resistivity of these lower hybrid modes is much smaller than that of the ion acoustic, because the long wavelength modes are much less effective at slowing down the electrons. Similarly, the heating rates associated with these modes are also smaller than those of the ion acoustic instability.

D. Other instabilities

We briefly discuss several other instabilities which have been considered in relation to heating at shocks.

1. Electron whistler instability. This mode is driven by a temperature anisotropy, $T_{e\perp}/T_{e\parallel}>1$ (Kennel and Petschek, 1966; Scharer and Trivelpiece, 1967) The instability condition is $T_{e\perp}/T_{e\parallel}>1+k^2c^2/\omega_e^2$; typically, $\omega_r \sim \gamma \sim \Omega_e$. The linear and nonlinear properties are well known (Ossakow et al, 1972). In the shock this mode can arise because of conservation of magnetic moment at the quasiperpendicular shock increases $T_{e\perp}$ (see Wu et al., 1984; review by Gurnett).

2. Electromagnetic ion cyclotron instability. This instability is similar to the previous, except that the anisotropy is in the ions. The linear and quasilinear properties ($\omega_r \sim \Omega_i$, $k_\parallel \sim \omega_i/c$, $\gamma \sim \Omega_i(\beta_{i\perp}/2)^{1/2}$). are found in Davidson and Ogden (1975); the nonlinear behavior has been simulated by Tajima et al. (1977). The instability provides a mechanism to isotropize the reflected ions when they gyrate downstream and permit some of them to escape along field lines back into the foreshock (Lee et al, 1981; Tanaka et al, 1983; review by Goodrich).

3. Whistler decay instability. This mode has been discussed briefly with respect to the ion-ion instability. It provides a means of producing short wavelength electrostatic turbulence (and a way to heat ions) at quasiparallel shocks (see review by Quest).

4. Beam driven ion acoustic instability. Within the shock ramp the electron velocity distribution parallel to the magnetic field often shows a beam-like protrusion on the ingoing edge of the developing flattop (e.g., Fig. 4). Linear analysis shows such distributions can be unstable to ion acoustic modes, which may play a role in heating and flattening of the electron distribution (Thomsen et al., 1983; Feldman review).

5. Lower hybrid and ion acoustic velocity ring distributions. The gyrating ions at supercritical quasiperpendicular shocks tend to form a ring-like velocity distribution, which can be unstable to a variety of modes (Wu et al., 1984). Such instabilities may explain some of the turbulence which is observed downstream of the main shock transition (Rodriguez and Gurnett, 1975; Formisano and Torbert, 1982).

IV. Conclusions

We conclude by reviewing the progress made over the last decade and summarizing the current status of our understanding of dissipation processes in collisionless shocks. During the last ten years the number of instabilities (theorists say) which can occur at shocks has

not grown appreciably, although how much we know about the various wave modes has increased a good deal. For example, in recent years linear analysis has become more sophisticated (improved calculations of VB effects) and has been applied to more realistic shock-like geometries (self-consistent equilibria with all gradients, inclusion of reflected ions for supercritical shocks). There have also been a number of new computer simulations of some of the instabilities (lower hybrid drift, kinetic cross-field streaming instabilities), which have led to a better understanding of their nonlinear behavior and which have been folded into calculations of their transport properties.

Even with the advances of the last decade, a number of key questions concerning microinstabilities remain unanswered. While the role of the ion acoustic instability for plasma heating at shocks when $T_e/T_i>>1$ remains undisputed, the issue of the dissipation mechanism for $T_e \approx T_i$ remains unsettled. The electron cyclotron drift instability is usually dismissed because of its low saturation level; but as has been discussed here, it has a nonlinear behavior which is not easily described and which depends in part on the geometry and the presence of turbulence. How important such effects are at the shock for the various instabilities (not just the electron cyclotron drift) is unknown. Another unanswered question concerns the origin of the strong heating of ions at laminar shocks with $T_e/T_i>>1$ (Fig. 2). Although in this case the ion acoustic instability is the natural candidate, it generally produces ion tails, rather than bulk heating. In this case, however, the principal evidence comes from simulations in idealized geometries with unmagnetized ions; again, the effect of the instability in the shock layer may be somewhat different. In these shocks beta is low enough that the ion heating rate due to the modified two stream instability is large enough to explain the observed heating (Thomsen et al., 1984). Simulations of such shocks (Forslund et al., 1983), however, do not show any evidence for wave growth or turbulent heating, even though it is predicted by linear theory and seen in the simulations at higher Mach numbers (Aldrich et al., 1983; Forslund et al., 1984).

The importance of the lower-hybrid-like modes at high beta is also not settled. While these instabilities can lead to significant heating at low beta (especially of ions) in laboratory experiments and simulations, their role at the bow shock is still unclear. Finite beta effects (which do not affect the shorter wavelength, electrostatic modes) stabilize the ion-ion instability, reduce the growth rates of the lower hybrid drift instability, and significantly lower the saturation level of the kinetic cross-field streaming instability. In addition, the heating rates of these modes seem too small to heat the ions very much at the bow shock, although they could generate (some) of the observed low frequency, electromagnetic noise.

There are a number of ways in which theory can be improved in order to resolve some of these questions over the next few years. For example, almost all of the linear analysis which has been done involves local theory. Although such calculations are valuable for determining under what conditions instabilities should be operative, it should be noted that nonlocal effects (e.g., Huba et al., 1980) can significantly modify the nature of some instabilities. What is needed most are some detailed linear calculations using measured plasma parameters and distribution functions, which are then compared to the actual wave observations.

Such improved linear analysis would also impact on better estimates of plasma heating at shocks due to the various instabilites. Further advances in transport calculations can be expected in the future. For example, nonlocal quasilinear theory is still in the embryonic stage (e.g., Sgro and Gladd, 1983) and will someday find application to shocks.

The best method for understanding microscopic processes at shocks remains computer simulation. The development of new implicit methods of particle simulation (Brackbill and Forslund, 1982) coupled with advances in the size and speed of computers allows the possibility of tackling problems on a scale that was impossible a decade ago. Generally the study of instabilities by simulation has involved the simplest of geometries. Such calculations need to be extended now to shock-like geometries to investigate the role of the nonlocal and nonlinear effects mentioned previously. Simulations of heating in laminar shocks at Los Alamos indicate some progress is being made in this area at the present time.

To sum up, the study of dissipation processes remains one of the most important research areas in collisionless shocks. In spite of a basic corsensus on the importance of instabilities and wave-particle interactions, a mature theory base, and recent advances in observations, theory and simulation, a number of fundamental questions remain unanswered.

Acknowledgements

I wish to thank Drs. Peter Gary, Michelle Thomsen, and Ching Wu for their comments and suggestions. This work was supported by the NASA Solar Terrestrial Theory Program and the Dept. of Energy.

References

Aldrich, C. H., J. U. Brackbill, D. W. Forslund, K. Lee, K. B. Quest, and D. Winske, Wave turbulence in quasiperpendicular shocks, EOS Trans., 64, 824, 1983.

Auer, P. L., R. W. Kilb, and W. F. Crevier, Thermalization in the earth's bow shock, J. Geophys. Res., 76, 2927, 1971.

Biskamp, D. and R. Chodura, Computer simulation of anomalous dc resistivity, Phys. Rev. Lett., 27, 1553, 1971.

Biskamp, D. and R. Chodura, On the nonlinear electron cyclotron drift instability, Nucl. Fusion, 12, 485, 1972.

Biskamp, D. and H. Welter, Structure of the earth's bow shock, J. Geophys. Res., 77, 6052, 1972.

Biskamp, D., Collisionless shock waves in plasmas, Nucl. Fusion, 13, 719, 1973.

Biskamp, D. and R. Chodura, Collisionless dissipation of a cross field electric current, Phys. Fluids, 16, 893, 1973.

Brackbill, J. U. and D. W. Forslund, An implicit method for electromagnetic plasma simulation in two dimensions, J. Comp. Phys., 46, 271, 1982.

Brackbill, J. U., D. W. Forslund, K. B. Quest, and D. Winske, Nonlinear evolution of the lower hybrid drift instability, Phys. Fluids, to be submitted, 1984.

Chen, Y.-J., W. M. Nevins, and C. K. Birdsall, Stabilization of the lower hybrid drift instability by resonant electrons, Phys. Fluids, 26, 2501, 1983.

Davidson, R. C., N. A. Krall, K. Papadopoulos, and R. Shanny, Electron heating by electron-ion beam instabilities, Phys. Rev. Lett., 24, 579, 1970.

Davidson, R. C. and N. T. Gladd, Anomalous transport properties associated with the lower hybrid drift instability, Phys. Fluids, 18, 1327, 1975.

Davidson, R. C. and J. M. Ogden, Electromagnetic ion cyclotron instability driven by ion energy anisotropy in high beta plasmas, Phys. Fluids, 18, 1045, 1975.

Davidson, R. C., N. T. Gladd, C. S. Wu, and J. D. Huba, Effects of finite plasma beta on the lower hybrid drift instability, Phys. Fluids, 20, 301, 1977.

Davidson, R. C. and N. A. Krall, Anomalous transport in high temperature plasmas with applications to solenoidal fusion systems, Nucl. Fusion, 17, 1313, 1977.

Drake, J. F., P. N. Guzdar, and J. D. Huba, Saturation of the lower hybrid drift instability by mode coupling, Phys. Fluids, 26, 601, 1983.

Drake, J. F., P. N. Guzdar, A. B. Hassam, and J. D. Huba, Nonlinear mode coupling theory of the lower hybrid drift instability, Phys. Fluids, 27, in press, 1984.

Dum, C. T., R. Chodura, and D. Biskamp, Turbulent heating and quenching of the ion sound instability, Phys. Rev. Lett., 32, 1231, 1974.

Dum, C. T., Anomalous heating by ion sound turbulence, Phys. Fluids, 21, 945, 1978a.

Dum, C. T., Anomalous electron transport equations for ion sound and related turbulent spectra, Phys. Fluids, 21, 956, 1978b.

Dum, C. T. and R. Chodura, Anomalous transition from Buneman to ion sound instability, in Wave Instabilities in Space Plasmas, edited by P. J. Palmadesso and K. Papadopoulos, p. 135, D. Reidel, 1979.

Feldman, W. C., R. C. Anderson, S. J. Bame, S. P. Gary, J. T. Gosling, D. J. McComas, M. F. Thomsen, G. Paschmann, and M. M. Hoppe, Electron velocity distributions near the earth's bow shock, J. Geophys. Res., 88, 96, 1983.

Feldman, W. C., Electron velocity distributions near collisionless shocks, Chapman conference on collisionless shocks, AGU, 1984.

Formisano, V. and R. Torbert, Ion acoustic waveforms generated by ion-ion streams at the earth's bow shock, Geophys. Res. Lett., 9, 207, 1982.

Forslund, D. W., R. L. Morse, and C. W. Nielson, Electron cyclotron drift instability, Phys. Rev. Lett., 25, 1266, 1970.

Forslund, D. W., R. L. Morse, and C. W. Nielson, Nonlinear electron cyclotron drift instability and turbulence, Phys. Rev. Lett., 27, 1424, 1971.

Forslund, D. W., J. M. Kindel, and E. L. Lindman, Parametric excitation of electromagnetic waves, Phys. Rev. Lett., 29, 249, 1972.

Forslund, D. W., K. B. Quest, C. H. Aldrich, J. U. Brackbill, and K. Lee, Simulation of subcritical collisionless shocks, EOS Trans., 64, 824, 1983.

Forslund, D. W., K. Quest, J. U. Brackbill, and K. Lee, Collisionless dissipation in quasiperpendicular shocks, J. Geophys. Res., 89, in press, 198-.

Freidberg, J. P. and R. A. Gerwin, Lower hybrid drift instability at low drift velocities, Phys. Fluids, 20, 1311, 1977.

Galeev, A. A., Collisionless shocks, in Physics of Solar Planetary Environments, edited by D. J. Williams, p. 464, AGU, 1976.

Gary, S. P., Wave-particle transport from electrostatic instabilities, Phys. Fluids, 23, 1193, 1980.

Gladd, N. T., The lower hybrid drift instability and the modified two stream instability in high density theta pinch environments, Plasma Phys., 18, 27, 1976.

Gold, S. H., A. W. DeSilva, and J. D. Huba, Observation of shock generated turbulence in a magnetized plasma by CO_2 laser scattering, Phys. Fluids, 23, 1132, 1980.

Goodrich, C. C., A review of numerical simulations of quasiperpendicular collisionless shocks, Chapman conference on collisionless shocks, AGU, 1984.

Greenstadt, E. W., and R. W. Fredricks, Plasma instability modes related to the earth's bow shock, in Magnetospheric Physics, edited by B. M. McCormac, p. 281, D. Reidel, 1974.

Greenstadt, E. W., V. Formisano, C. T. Russell, M. Neugebauer, and F. L. Scarf, Ion acoustic stability analysis of the earth's bow shock, Geophys. Res. Lett., 5, 399, 1978.

Greenstadt, E. W., and R. W. Fredricks, Shock systems in collisionless plasmas, in Solar System Plasma Physics, Edited by I. J. Lanzerotti, C. F. Kennel, and E. N. Parker, Vol. III, p. 5, North Holland, 1979.

Greenstadt, E. W., C. T. Russell, J. T. Gosling, S. J. Bame, G. Paschmann, G. K. Parks, K. A. Anderson, F. L. Scarf, R. R. Anderson, D. A. Gurnett, R. P. Lin, C. S. Lin, and H. Reme, A macroscopic profile of the typical quasiperpendicular bow shock: ISEE 1 and 2, J. Geophys. Res., 85, 2124, 1980.

Greenstadt, E. W., A review of the structure of the quasiparallel shock, Chapman conference on collisionless shocks, AGU, 1984.

Gurnett, D. A., Waves and instabilities at collisionless shocks, Chapman conference on collisionless shocks, AGU, 1984.

Hamasaki, S., N. A. Krall, C. E. Wagner, and R. N. Byrne, Effect of turbulence on theta pinch modeling by hybrid numerical methods, Phys. Fluids, 20, 65, 1977.

Hasegawa, A., Plasma Instabilities and Nonlinear Effects, Springer-Verlag, 1975.

Horton, W., D. Choi, and R. A. Koch, Ion acoustic heating from renormalized turbulence theory, Phys. Rev., A14, 424, 1976.

Horton, W., D. Choi, and R. A. Koch, Scaling law and asymptotic states for ion acoustic turbulence, Phys. Fluids, 22, 797, 1979.

Hsia, J. B., S. M. Chiu, M. F. Hsia, R. L. Chou, and C. S. Wu, Generalized lower hybrid drift instability, Phys. Fluids, 22, 1737, 1979.

Huba, J. D., J. F. Drake, and N. T. Gladd, Lower hybrid drift instability in field reversed plasmas, Phys. Fluids, 23, 552, 1980.

Huba, J. D., N. T. Gladd, and J. F. Drake, On the role of the lower hybrid drift instability in substorm dynamics, J. Geophys. Res., 86, 5881, 1981.

Kadomsev, B. B., Plasma Turbulence, Academic, 1965.

Kennel, C. F. and H. E. Petschek, Limit on stably trapped particle fluxes, J. Geophys. Res., 71, 1, 1966.

Kennel, C. F., An overview of collisionless shocks, Chapman conference on collisionless shocks, AGU, 1984.

Klimas, A., A review of the electron foreshock, Chapman conference on collisionless shocks, AGU, 1984.

Krall, N. A. and P. C. Liewer, Low frequency instabilities in magnetic pulses, Phys. Rev., A4, 2094, 1971.

Krall, N. A. and A. W. Trivelpiece, Principles of Plasma Physics, McGrall Hill, 1973.

Lampe, M., W. M. Manheimer, J. B. McBride, J. H. Orens, R. Shanny, and R. N. Sudan, Nonlinear development of the beam cyclotron instability, Phys. Rev. Lett., 26, 1221, 1971.

Lampe, M., W. M. Manheimer, J. B. McBride, J. H. Orens, K. Papadopoulos, R. Shanny, and R. N. Sudan, Theory and simulation of the beam cyclotron instability, Phys. Fluids, 15, 662, 1972a.

Lampe, M., W. M. Manheimer, J. B. McBride, and J. H. Orens, Anomalous resistance due to cross-field electron-ion streaming instabilities, Phys. Fluids, 15, 2356, 1972b.

Lampe, M., I. Haber, J. H. Orens, and J. P. Boris, Two-dimensional study of electron-ion streaming instabilities, Phys. Fluids, 17, 428, 1974.

Lampe, M.,W. M. Manheimer, and K. Papadopoulos, Anomalous transport coefficients for HANE applications due to plasma microinstabilities, NRL Memorandum Report 3076, 1975.

Lashmore-Davies, C. N., and T. J. Martin, Electrostatic instabilities driven by an electric current perpendicular to a magnetic field, Nucl. Fusion, 13, 193, 1973.

Lee, K., J. U. Brackbill, D. W. Forslund, and K. Quest, Dissipation of reflected ion beams from quasiperpendicular shocks due to electromagnetic ion cyclotron instability, EOS Trans., 62, 1011, 1981.

Lemons, D. S. and S. P. Gary, Electromagnetic effects on the modified two stream instability, J. Geophys. Res., 82, 2337, 1977.

Lemons, D. S. and S. P. Gary, Current-driven instabilities in a laminar perpendicular shock, J. Geophys. Res., 83, 1625, 1978.

Leroy, M. M., D. Winske, C. C. Goodrich, C. S. Wu, and K. Papadopoulos, The structure of perpendicular bow shocks, J. Geophys. Res., 87, 5081, 1982.

Leroy, M. M. and D. Winske, Backstreaming ions from oblique earth bow shocks, Annales Geophys., 1, 527, 1983.

Liewer, P. C. and N. A. Krall, Self-consistent approach to anomalous resistivity applied to theta-pinch experiments, Phys. Fluids, 16, 1953, 1973.

Liewer, P. C., Numerical studies of ion reflection in collisionless theta-pinch implosions using a hybrid Vlasov fluid model, Nucl. Fusion, 16, 817, 1976.

Manheimer, W. M. and J. P. Boris, Self-consistent theory of a collisionless, resistive shock, Phys. Rev. Lett., 28, 659, 1972.

McBride, J. B. and E. Ott, Electromagnetic and finite β_e effects on the modified two stream instability, Phys. Lett, 39A, 363, 1972.

McBride, J. B., E. Ott, J. P. Boris, and J. H. Orens, Theory and simulation of turbulent heating by the modified two stream instability, Phys. Fluids, 15, 2367, 1972.

Morse, D. L. and E. W. Greenstadt, Thickness of magnetic structures associated with the earth's bow shock, J. Geophys. Res., 81, 1791, 1976.

Morse, R. L. and C. W. Nielson, Studies of turbulent heating of hydrogen plasmas by numerical simulation, Phys. Rev. Lett., 26, 3, 1971.

Ossakow, S. L., E. Ott, and I. Haber, Nonlinear evolution of whistler instabilites, Phys. Fluids, 15, 2314, 1972.

Papadopoulos, K., Ion thermalization in the earth's bow shock, J. Geophys. Res., 76, 3806, 1971.

Papadopoulos, K., R. C. Davidson, J. M. Dawson, I. Haber, D. A. Hammer, N. A. Krall, and R. Shanny, Heating of counterstreaming ion beams in an external magnetic field, Phys. Fluids, 14, 849, 1971.

Papadopoulos, K., A review of anomalous resistivity for the ionosphere, Rev. Geophys. Space Phys., 15, 113, 1977.

Papadopoulos, K., Microphysics of collisionless shocks, Chapman conference on collisionless shocks, AGU, 1984.

Priest, E. R. and J. J. Sanderson, Ion acoustic instability in collisionless shocks, Plasma Phys., 14, 951, 1972.

Quest, K. B., D. W.Forslund, J. U. Brackbill, and K. Lee, Collisionless dissipation processes in quasiparallel shocks, Geophys. Res. Lett., 10, 471, 1983.

Quest, K. B., A review of the simulations of quasiparallel collisionless shocks, Chapman conference on collisionless shocks, AGU, 1984.

Revathy, P. and G. S. Lakina, Ion and electron heating in the earth's bow shock region, J. Plasma Phys., 17, 133, 1977.

Robson, A. E., A review of the evolution of ion distributions across collisionless shocks in the laboratory and space, Chapman conference on collisionless shocks, AGU, 1984.

Rodriguez, P. and D. A. Gurnett, Electrostatic and electromagnetic turbulence associated with the earth's bow shock, J. Geophys. Res., 80, 19, 1975.

Rodriguez, P. and D. A. Gurnett, Correlation of bow shock plasma wave turbulence with solar wind parameters, J. Geophys. Res., 81, 2871, 1976.

Russell, C. T., M. M. Hoppe, W. A. Livesey, J. T. Gosling, and S. J. Bame, ISEE-1 and 2 observations of laminar bow shocks: velocity and thickness, Geophys. Res. Lett., 9, 1171, 1982.

Sagdeev, R. Z. and A. A. Galeev, Nonlinear Plasma Theory, Benjamin, 1969.

Scharer, J. E. and A. W. Trivelpiece, Cyclotron wave instabilities in a plasma, Phys. Fluids, 10, 591, 1967.

Sckopke, N., G. Paschmann, S. J. Bame, J. T. Gosling, and C. T. Russell, Evolution of ion distributions across the nearly perpendicular bow shock: specularly and nonspecularly reflected ions, J. Geophys. Res., 88, 6121, 1983.

Sgro, A. G., Calculations of the effects of incomplete preionization in high voltage theta pinches, Phys. Fluids, 21, 1410, 1978.

Sgro, A. G. and N. T. Gladd, The lower hybrid drift instability near the separatrix of a field reversed configuration, Bull. A.P.S., 28, 1244, 1983.

Sleeper, A. M., J. Weinstock, and B. Bezzerides, Nonlinear theory and angular spectrum of the ion acoustic instability, Phys. Fluids, 16, 1508, 1973.

Soldner, F., C. T. Dum, and K. -H. Steuer, Electron and ion heating in a high voltage belt pinch, Phys. Rev. Lett., 39, 194, 1977.

Tajima, T., K. Mima, and J. M. Dawson, Alfven ion cyclotron instability: its physical mechanism and observation in computer simulation, Phys. Rev. Lett., 39, 201, 1977.

Tanaka, M. and T. Sato, Simulations of lower hybrid drift instability and anomalous resistivity in the magnetic neutral sheet, J. Geophys. Res., 86, 5541, 1981.

Tanaka, M., C. C. Goodrich, D. Winske, and K. Papadopoulos, A source of the backstreaming ion beams in the foreshock region, J. Geophys. Res., 88, 3046, 1983.

Thomsen, M. L., H. C. Barr, S. P. Gary, W. C. Feldman, and T. E. Cole, Stability of electron distributions within the earth's bow shock, J. Geophys. Res., 88, 3035, 1983.

Thomsen, M. L., A review of superthermal ions and related waves in the ion foreshock, Chapman conference on collisionless shocks, AGU, 1984.

Thomsen, M. L., J. T. Gosling, S. J. Bame, and M. M. Mellott, Ion and electron heating at the subcritical bow shock, J. Geophys. Res., to be submitted, 1984.

Tidman, D. A. and N. A. Krall, Shock Waves in Collisionless Plasmas, Wiley, 1971.

Tsai, S. T., M. Tanaka, J. D. Gaffey, E. H. da Jornada, and C. S. Wu, Effect of electron thermal anisotropy on the kinetic cross-field streaming instability, Phys. Fluids, 27, in press, 1984.

Tsytovich, V. N., An Introduction to the Theory of Plasma Turbulence, Pergamon, 1972.

Wagner, C. E., K. Papadopoulos, and J. Huber, Electromagnetic and finite β_e effects on the counterstreaming ion instability, Phys. Lett., 35A, 440, 1971.

Wesson, J. A. and A. Sykes, Theory of ion sound resistivity, Phys. Rev. Lett., 31, 449, 1973.

Winske, D. and P. C. Liewer, Particle simulation studies of the lower hybrid drift instability, Phys. Fluids, 21, 1017, 1978.

Winske, D., Simulation of the lower hybrid drift instability, U. of Maryland Plasma Preprint PL 82-001, 1981.

Winske, D., M. Tanaka, and C. S. Wu, Plasma heating due to the kinetic cross-field streaming instability, Phys. Fluids, to be submitted, 1984.

Wu, C. S. and R. W. Fredricks, Cyclotron drift instability in the bow shock, J. Geophys. Res., 77, 5585, 1972.

Wu, C. S., Physical mechanisms for turbulent dissipation in collisionless shock waves, Space Sci. Rev., 32, 83, 1982.

Wu., C. S., Y. M. Zhou, S. T. Tsai, S. C. Cuo, D. Winske, and K. Papadopoulos, A kinetic cross-field streaming instability, Phys. Fluids, 26, 1259, 1983.

Wu, C. S., D. Winske, Y. M. Zhou, S. T. Tsai, P. Rodriguez, M. Tanaka, K. Papadopoulos, A. Akimoto, C. S. Lin, M. M. Leroy, and C. C. Goodrich, Microinstabilities associated with a high Mach number perpendicular bow shock, Space Sci. Rev., 36, in press, 1984.

Zhou, Y. M., H. K. Wong, C. S. Wu, and D. Winske, Lower hybrid drift instability with temperature gradient in a perpendicuar shock wave, J. Geophys. Res., 88, 3026, 1983.

Zhou, Y. M., Y. Y. Li, and C. S. Wu, Stabilization of electron cyclotron drift instability by magnetic field gradient in a perpendicular shock wave, Phys. Fluids, 27, submitted, 1984.

Figure captions

Figure 1 Geometry of a perpendicular shock showing the field structure and sources of free energy (Wu, 1982).

Figure 2 Bow shock crossing of August 27, 1978 showing electron (solid curve) and ion (dashes and circles) densities, flow speed, and ion and electron temperatures (max and min) (Thomsen, et al., 1984).

Figure 3 Bow shock crossing of November 7, 1977 showing electron and reflected ion densities, proton and electron temperatures, flow speed, electron pressure, magnetic field magnitude and orientation (Sckopke, et al., 1983).

Figure 4 Evolution of the electron velocity distribution across the bow shock for the December 13, 1977 crossing from upstream (BS) to downstream (MS) (Feldman et al., 1983).

Figure 5 Electric field spectrum at 6 sec intervals through the shock crossing of Nov. 7, 1977 (from Wu. et al., 1984).

Figure 6 Kinetic cross field streaming instability: real (solid curves) and imaginary (dashed curves) parts of the frequency of the most unstable mode (maximized over k) versus propagation angle θ for various values of v_d/v_A (Tsai et al., 1984).

Figure 7 Heating rates ($\Lambda_\alpha=(\omega_{LH}T_\alpha)^{-1}dT_\alpha/dt$) versus β_i for the kinetic cross-field streaming instability (Winske et al., 1984).

Figure 8 Lower hybrid drift instability: growth rate maximized over wavenumber versus propagation angle θ for various values of the electron temperature gradient (Zhou et al., 1983).

Figure 9 Simulation results for a high Mach number quasiperpendicular shock (from Aldrich et al., 1983; Forslund et al., 1984): (a) phase space showing reflected ions, (b) magnetic field profile, (c) contour plot of electric field (E_y) at X=12.5, (d) E_y at X=12.5.

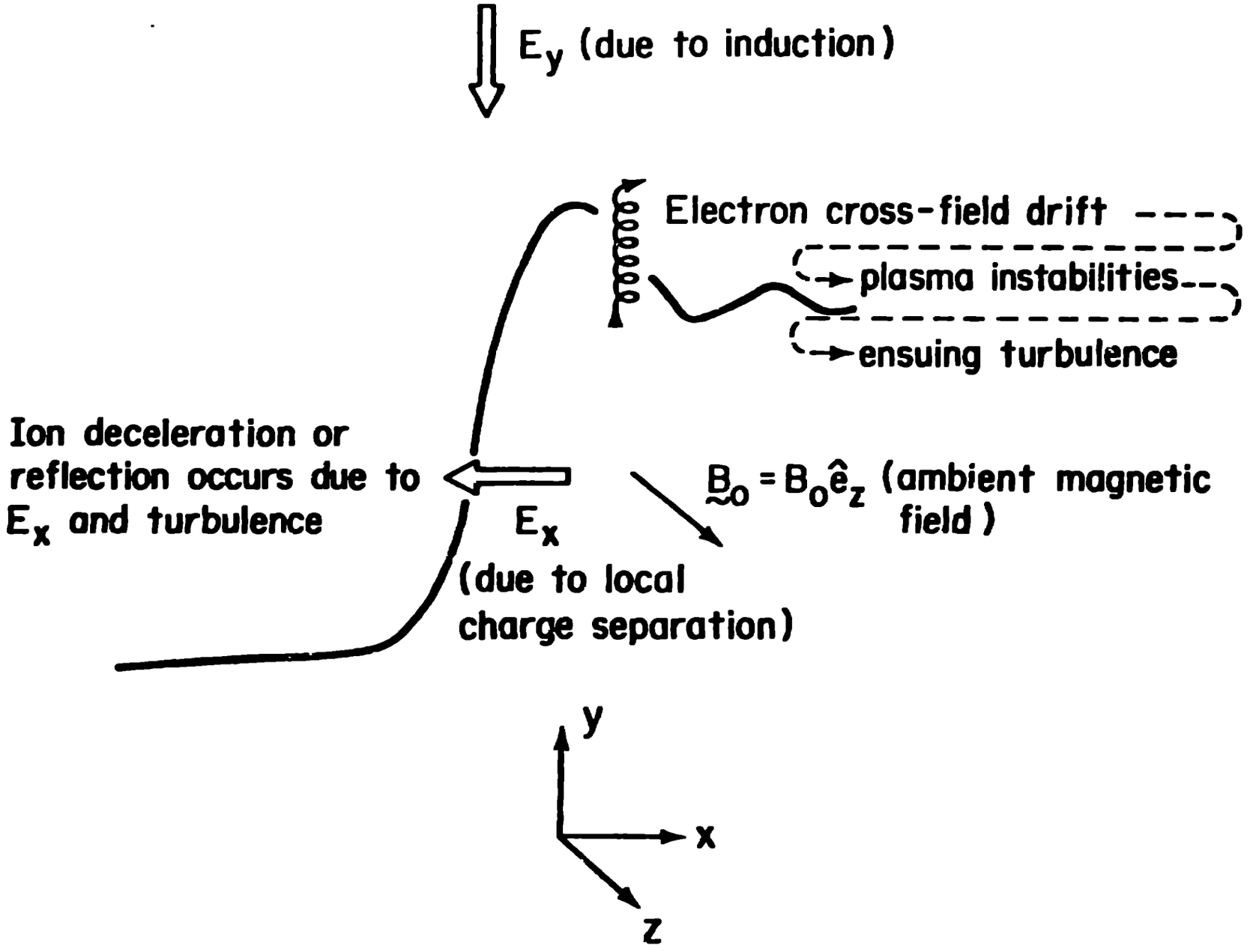
E_y (due to induction)
Electron cross-field drift
plasma instabilities
ensuing turbulence
Ion deceleration or reflection occurs due to E_x and turbulence
E_x
(due to local charge separation)
$\underset{\sim}{B}_o = B_o \hat{e}_z$ (ambient magnetic field)
y
x
z

Figure 1

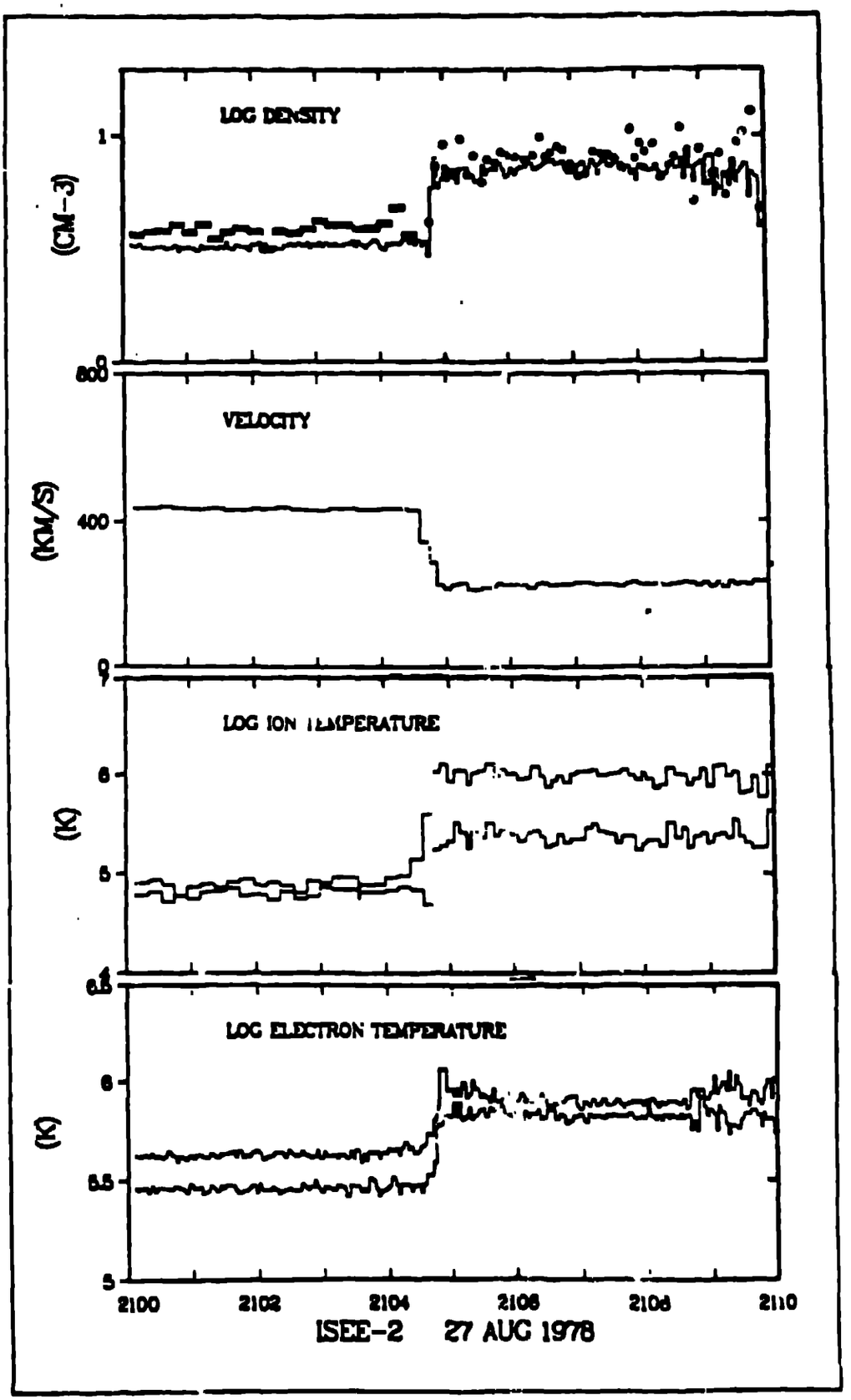
LOG DENSITY
(CM-3)
1
VELOCITY
(KM/S)
800
400
0
LOG ION TEMPERATURE
(K)
6
5
LOG ELECTRON TEMPERATURE
(K)
6
5.5
5
2100
2102
2104
2106
2108
2110
ISEE-2 27 AUG 1978

Figure 2

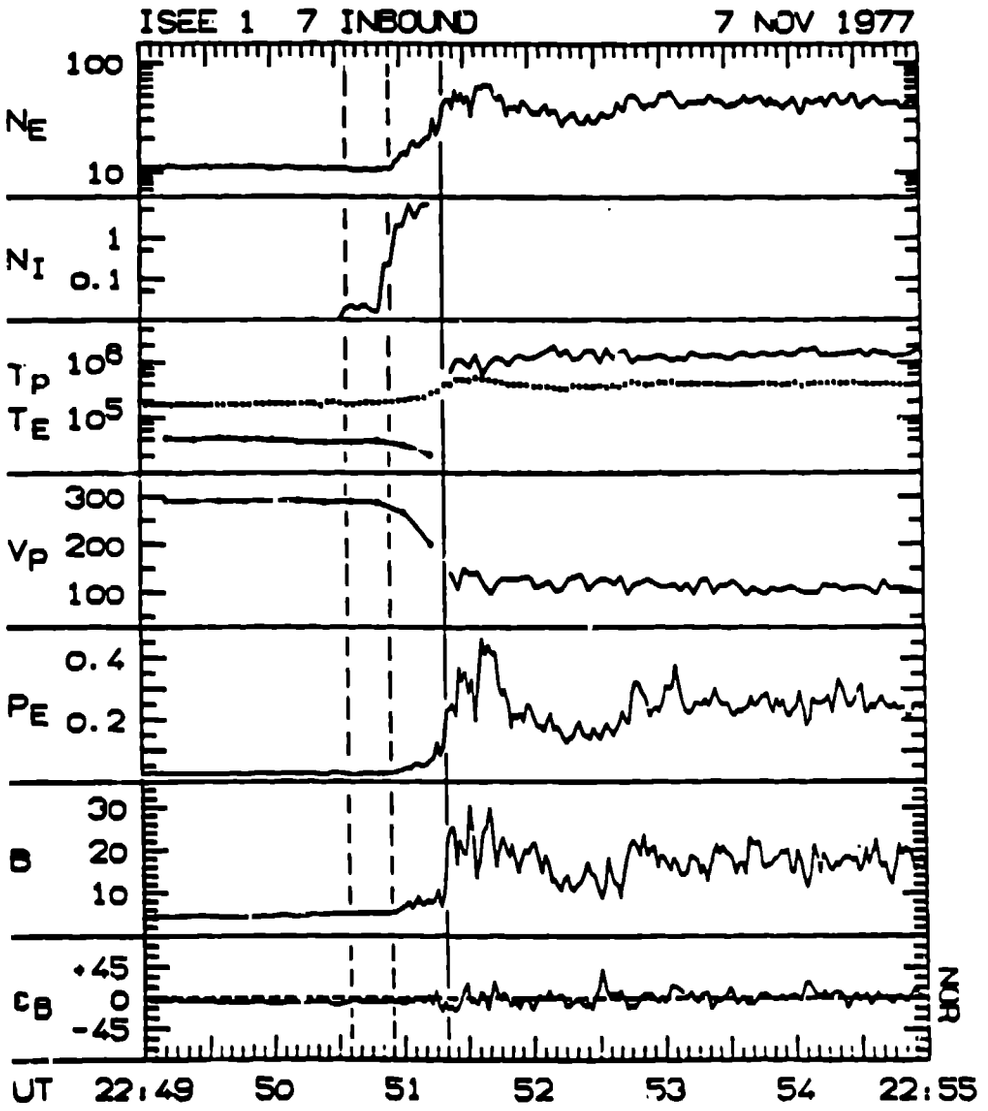
ISEE 1 7 INBOUND
7 NOV 1977
100
N_E
10
1
N_I
0.1
10^6
T_P
T_E 10^5
300
V_P 200
100
0.4
P_E 0.2
30
B 20
10
+45
α_B 0
-45
NOR
UT 22:49 50 51 52 53 54 22:55

Figure 3

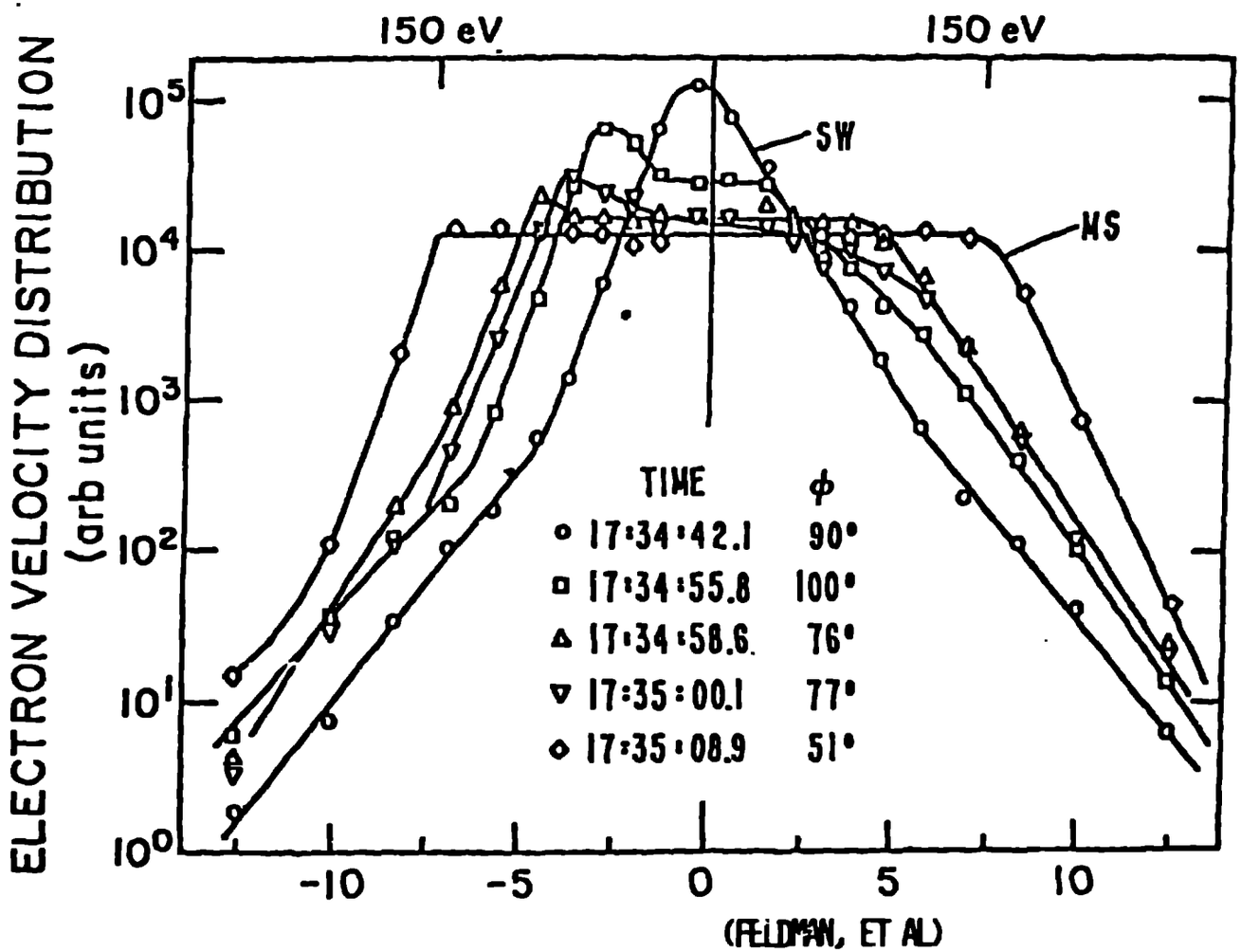
150 eV
150 eV
ELECTRON VELOCITY DISTRIBUTION
(arb units)
10^5
10^4
10^3
10^2
10^1
10^0
SW
MS
TIME
ϕ
○ 17:34:42.1 90°
□ 17:34:55.8 100°
△ 17:34:58.6 76°
▽ 17:35:00.1 77°
◇ 17:35:08.9 51°
-10
-5
0
5
10
(FELDMAN, ET AL)

Figure 4

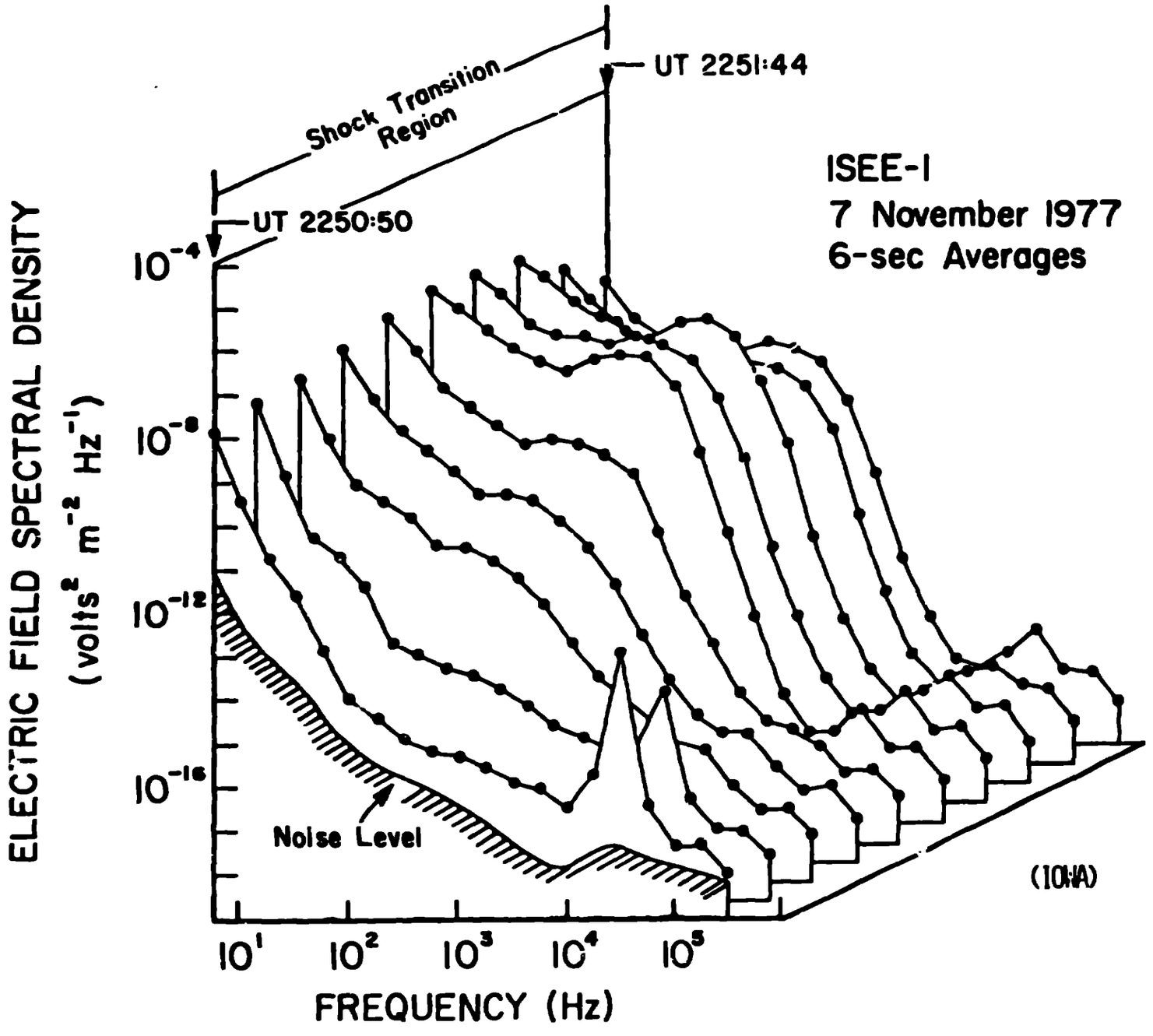
Shock Transition Region
UT 2251:44
UT 2250:50
ISEE-1
7 November 1977
6-sec Averages
ELECTRIC FIELD SPECTRAL DENSITY
(volts² m⁻² Hz⁻¹)
10⁻⁴
10⁻⁸
10⁻¹²
10⁻¹⁶
Noise Level
(10:A)
10¹
10²
10³
10⁴
10⁵
FREQUENCY (Hz)

Figure 5

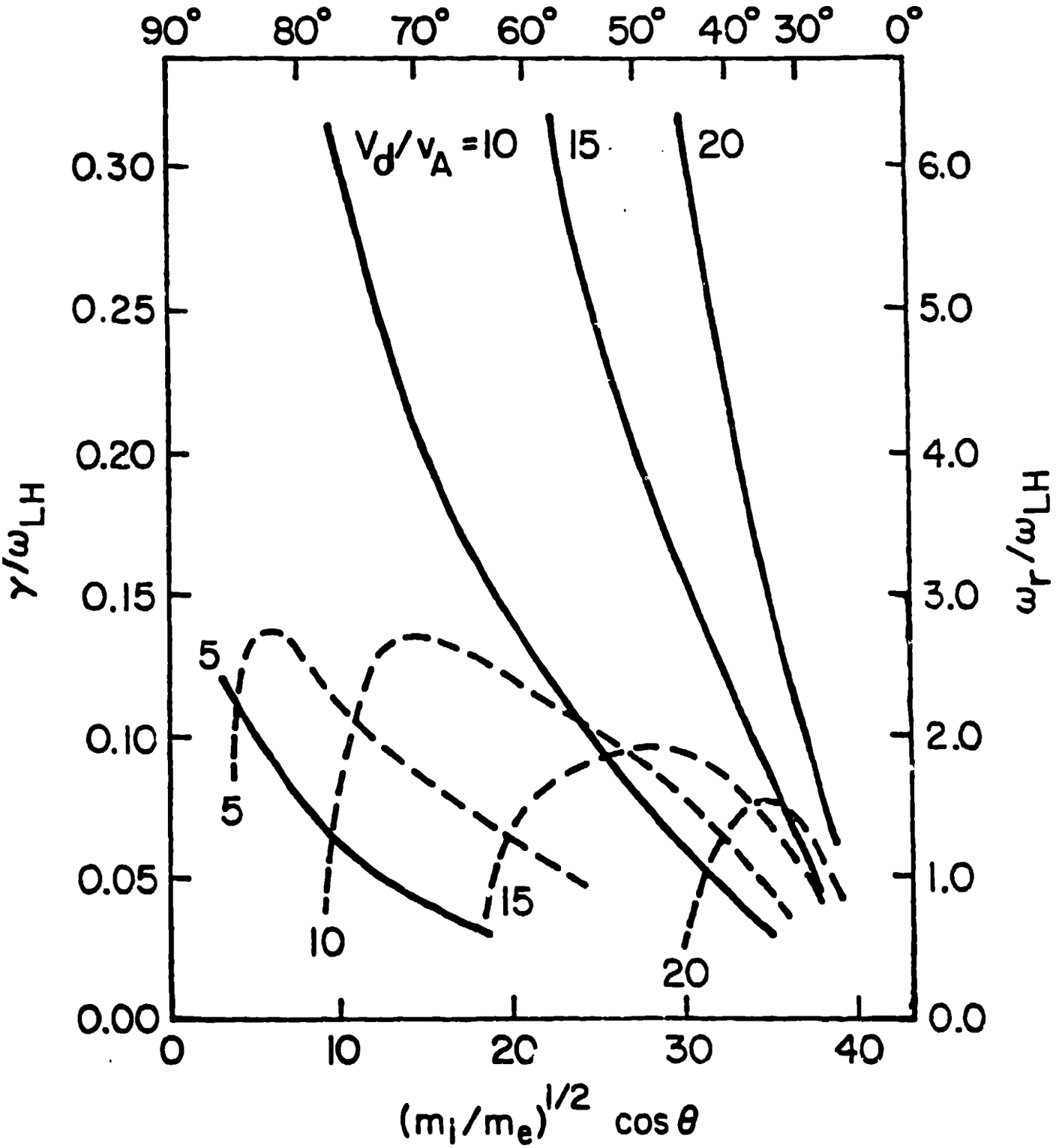
90°
80°
70°
60°
50°
40°
30°
0°
V_d/V_A =10
15
20
0.30
0.25
0.20
0.15
0.10
0.05
0.00
6.0
5.0
4.0
3.0
2.0
1.0
0.0
γ/ω_{LH}
ω_r/ω_{LH}
5
5
10
15
20
0
10
20
30
40
$(m_i/m_e)^{1/2}\cos\theta$

Figure 6

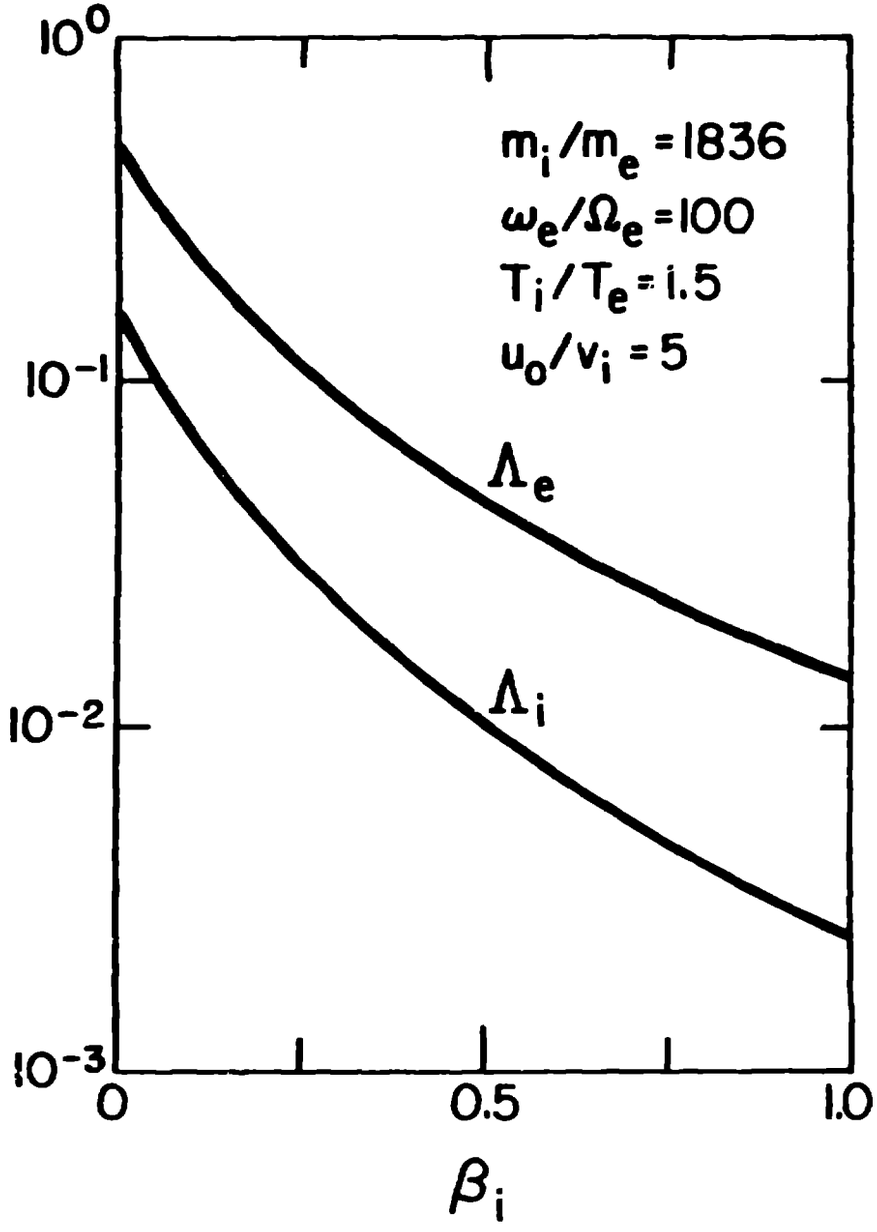
10^0
10^{-1}
10^{-2}
10^{-3}
$m_i/m_e = 1836$
$\omega_e/\Omega_e = 100$
$T_i/T_e = 1.5$
$u_o/v_i = 5$
Λ_e
Λ_i
0
0.5
1.0
β_i

Figure 7

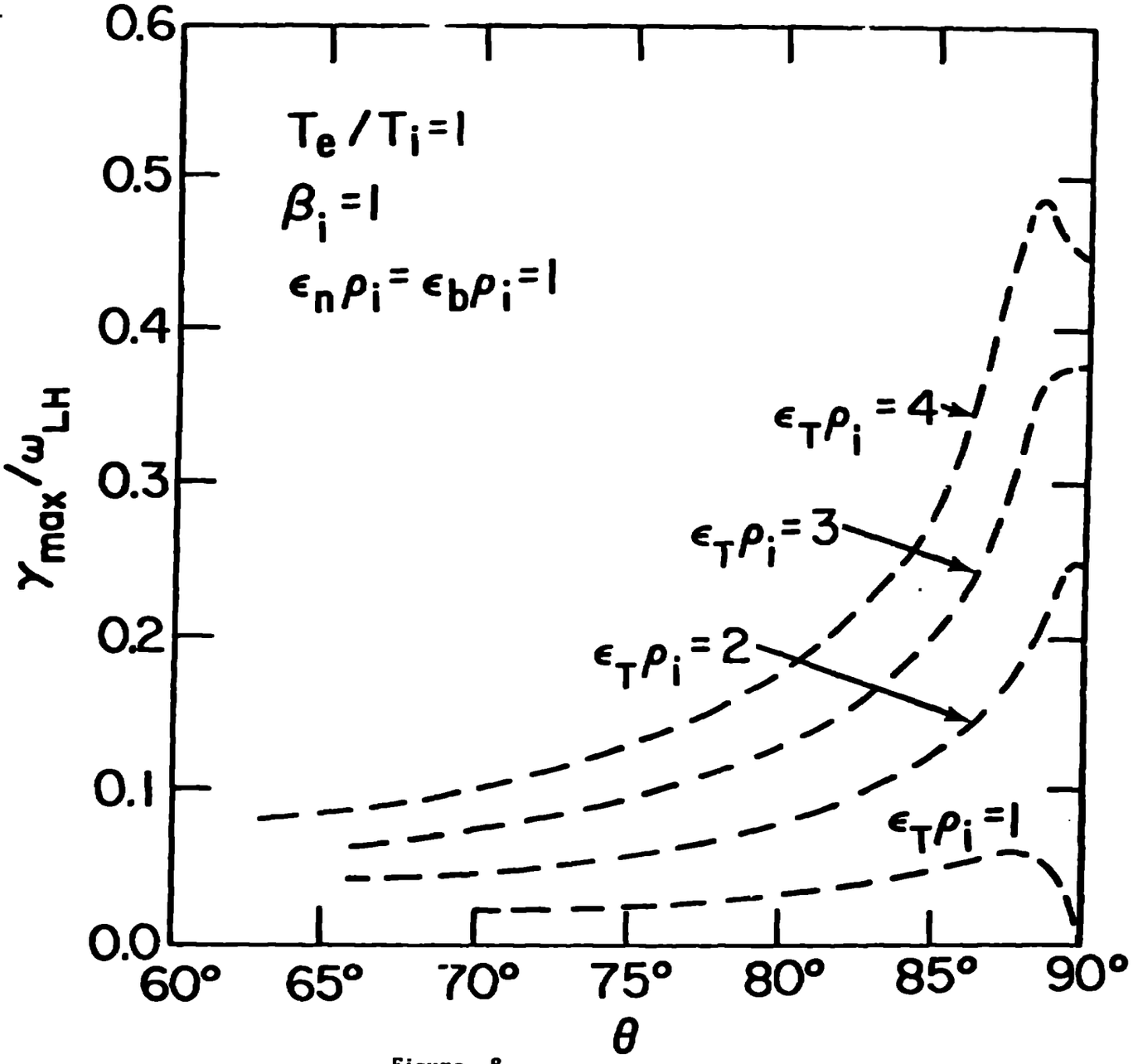
0.6
0.5
0.4
0.3
0.2
0.1
0.0
γ_{max}/ω_{LH}
$T_e/T_i=1$
$\beta_i=1$
$\epsilon_n\rho_i=\epsilon_b\rho_i=1$
$\epsilon_T\rho_i=4$
$\epsilon_T\rho_i=3$
$\epsilon_T\rho_i=2$
$\epsilon_T\rho_i=1$
60°
65°
70°
75°
80°
85°
90°
θ

Figure 8

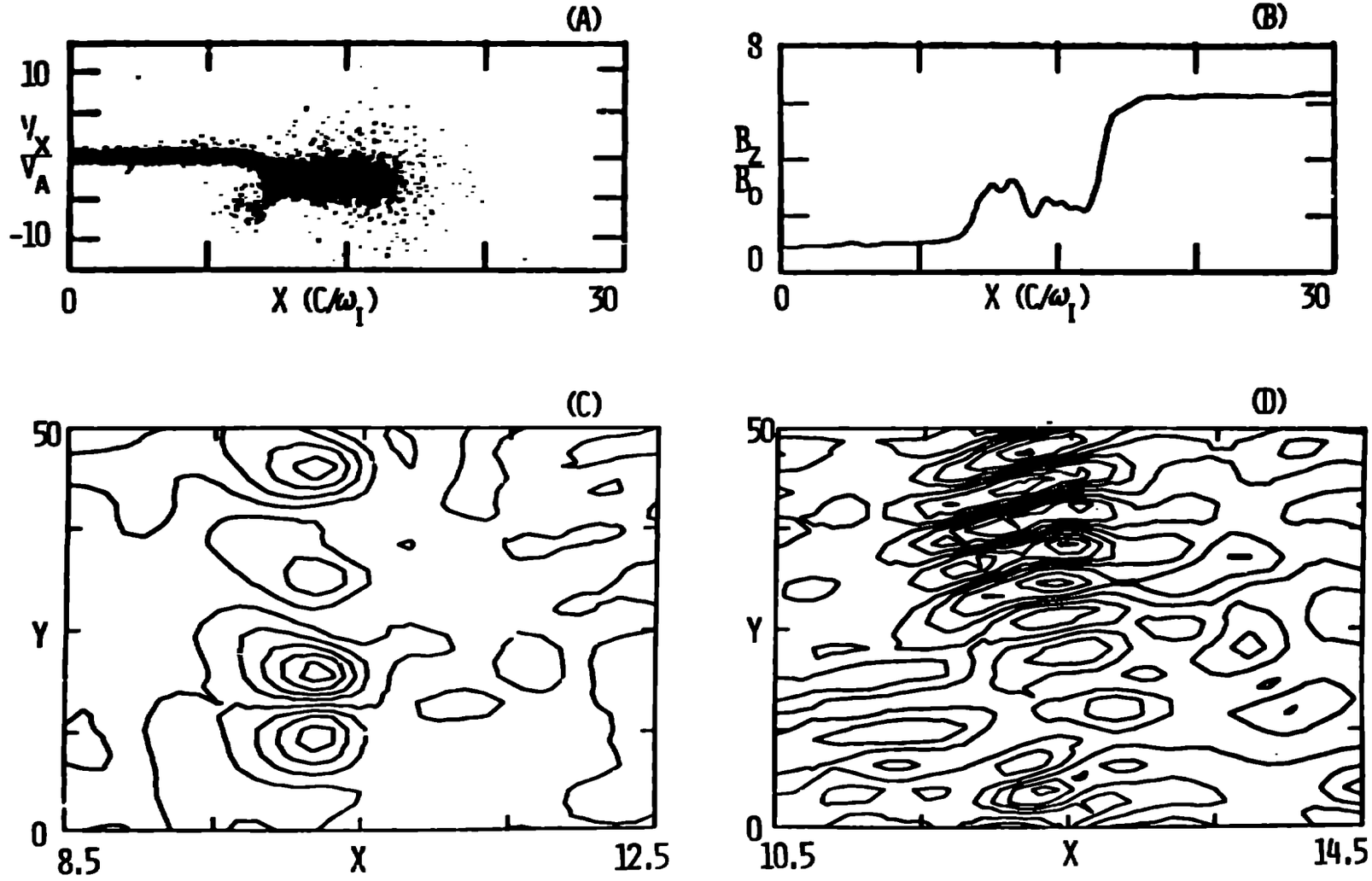
(A)
10
V_x/V_A
-10
0
X (C/ω_i)
30
(B)
8
B_z/B_0
0
0
X (C/ω_i)
30
(C)
50
Y
0
8.5
X
12.5
(D)
50
Y
0
10.5
X
14.5

Figure 9